THE MECHANICS OF FILM COOLING

Thesis by

Eldon L. Knuth

In Partial Fulfillment of the Requirements

For the Degree of

Doctor of Philosophy

California Institute of Technology

Pasadena, California

1954

ACKNOWLEDGMENTS

The author wishes to express his appreciation to Dr. W. Duncan Rannie for his critical guidance during the course of the study described herein.

The author is grateful for the many assistances given him by the staff members of the Jet Propulsion Laboratory, California Institute of Technology, where the major part of the work was carried out. Mr. N. Van De Verg, Chief of the Liquid Rockets Section, under whose general direction the research was performed, showed a continued interest in and gave indispensable support to the investigation.

The author is also grateful for the financial assistance afforded him by the Daniel and Florence Guggenheim Foundation in the form of a Fellowship in Jet Propulsion during the 1950-51 and 1951-52 school years.

ABSTRACT

Thin liquid wall films flowing under the influence of high-velocity turbulent gas streams were studied for the purpose of obtaining an understanding of the mechanics of film cooling. Conditions which insure liquid-film attachment to solid surfaces without loss of unevaporated liquid to the gas stream when simple radial-hole injectors are used were found; the maximum allowable coolant-flow rate for a stable coolant film was determined (a stable coolant film is obtained when no unevaporated coolant is entrained by the gas stream as the result of interfacial disturbances); and a method for calculating the evaporation rate and the surface temperature for a stable inert coolant film was found.

TABLE OF CONTENTS

SUMMARY

Thin liquid wall films flowing under the influence of high-velocity, turbulent gas streams were studied for the purpose of obtaining an understanding of the mechanics of film cooling. The problem was divided into three parts: (a) the determination of sufficient conditions for the attachment of liquid films to solid surfaces in the presence of high-velocity gas streams without entrainment of unevaporated liquid by the gas stream, (b) the determination of sufficient conditions for the stability of thin liquid wall films flowing under the influence of high-velocity turbulent gas streams (a stable film is a film which loses no liquid droplets to the adjacent gas stream as the result of surface disturbances), and (c) the determination of the evaporation rate from a stable inert liquid wall film into a heated turbulent gas stream.

Previous systematic studies of the liquid-film-attachment problem have been limited to the experimental studies by Zucrow et al on film attachment using an injection slot around a duct circumference in conjunction with the effects of a high-velocity gas stream. Former studies of the film-stability problem were also limited in scope; available reports (the most comprehensive being that by Kinney and Abramson) consist principally of descriptions of observed liquid-film surfaces for various flow conditions and discussions of mass-transfer data which indirectly reflect the condition of the liquid-film surface. The evaporation problem has been studied both theoretically and experimentally, however; e.g., Crocco has extended Rannie's approximate theory of porous-wall cooling for inert coolants

to porous-wall, sweat, and film cooling for the case in which the coolant itself is reactive with the hot gas stream, whereas Kinney has experimentally investigated liquid-film cooling with water in straight pipes through which heated turbulent air streams were flowing.

Studies reported here on liquid-film attachment indicated that the use of radial-hole injectors in conjunction with the effects of a high-velocity gas stream for the attachment of liquid films to solid surfaces is effective over a wide range of operating conditions. Data corresponding to the inception point of inefficient film attachment (inefficient attachment occurring when liquid droplets are entrained by the gas stream during the attachment process) were plotted in dimensionless form; the abscissa was a function of the gas-stream Reynolds number, the liquid-stream Reynolds number, and a modified cavitation parameter, and the ordinate was the ratio of the gas- and liquid-stream momenta.

The studies on liquid-film stability led to the conclusions that small disturbances with wavelengths of the order of 10 film thicknesses are present on the liquid-film surface for all liquid-flow rates, that the scale of the small disturbances decreases as the diameter Reynolds number of the gas stream increases but does not vary appreciably when the liquid-flow rate is changed, that long-wavelength disturbances appear on the surface of the film for liquid-flow rates larger than some critical value, that the critical film thickness for long-wavelength disturbances depends primarily on the wall shear stress, and that liquid droplets

are entrained by the gas stream from the crests (regions where relatively large quantities of liquid are collected) of the long-wavelength disturbances. Obviously, the unstable long-wavelength disturbances are to be avoided when designing for an efficient film-cooling system. The data corresponding to the inception point of unstable liquid-wall-film flows are presented in dimensionless form by plotting the dimensionless film thickness corresponding to the inception point of unstable liquid-wall-film flows as a function of the ratio of the gas-vapor-mixture viscosity to the liquid viscosity, where the viscosities were evaluated at the liquid-film surface temperature.

A theoretical analysis of the evaporation problem was based on an extension of the Reynolds analogy to heat, mass, and momentum transfer in the turbulent core of two-component fully developed turbulent pipe flow with unidirectional radial diffusion and on subsequent extensions of the Prandtl-Taylor equation to heat transfer and mass transfer in the case of film cooling. The resulting pair of equations, taken together, permits the calculation of the evaporation rate and the surface temperature for a liquid film when the fluid properties and gas-stream parameters are known.

Experimentally determined evaporation rates were brought into agreement with calculated evaporation rates after corrections for entrance effects were made. Good agreement was realized between predicted and measured film temperatures.

I. INTRODUCTION

I-A: Film Cooling and Its Uses[a]

Film cooling is the protection of a given surface from injurious effects of a proximate heated fluid stream by the interposing of a thin continuous protective liquid film between the given surface and the fluid stream. Its use is justified when the proximate fluid stream is extremely hot and when a more satisfactory method for protecting the given surface from destruction by heat is not available; or when the proximate fluid stream reacts chemically with the given surface, when such chemical reaction is undesirable, and when a more satisfactory method for separating the injurious fluid stream from the given surface is not available; or when the proximate fluid stream carries with it materials which are easily deposited on solid surfaces and when deposits of this nature are undesirable on the given surface. Structural members which are likely to be film-cooled include combustion chambers, where the heated fluids are the products of combustion, and external surfaces of high-velocity missiles, where the heated fluids are aerodynamically heated atmospheric gases. Inability to cool these structural members adequately could seriously limit the performance of the corresponding machines.

Important factors which should be considered before deciding

---

[a]Although the flow of thin liquid wall films under the influence of high-velocity turbulent gas streams and/or the unidirectional turbulent diffusion of one gas through another gas occurs in numerous engineering applications (e.g., in evaporators, condensers, two-phase combustion processes, and film-cooling systems), attention will be concentrated, for the sake of convenience, on that application which motivated the present study -- film-cooling systems.

to use film cooling as the solution to a given cooling problem in preference to (or in conjunction with) other cooling methods are the performance and the cost of the finished product. High performance frequently requires the cooling system to be designed so that high working pressures and temperatures can be tolerated and the finished product will be light in weight and small in size. Low cost is usually obtained if materials and coolants used are relatively inexpensive and if fabrication of the product is relatively simple.

In order to exemplify these comments, consider the cooling problems involved in the design of a liquid-propellant rocket motor[a] which is to propel a long-range missile. Experience indicates that one should design for combustion-chamber pressures of the order of 1000 psia, combustion temperatures of the order of 6000°R, and burning periods of the order of several minutes. Experience has also shown that the use of heat-capacity motors (motors in which the walls are thick enough to absorb the heat transferred to them during the running period without structural failure) is not feasible for these operating conditions. Thus one is left with the following two possible solutions to the cooling problem: (a) Remove heat from the outer surface of the motor wall as rapidly as heat is transferred from the combustion gases to the inner surface of the motor wall. This process is usually accomplished by passing a relatively cool liquid having a reasonably large heat capacity (frequently one of the propellants) over the outer surface of the motor wall. If the

---

[a]Historical note: It is believed that credit for the first application of film cooling is due Robert H. Goddard, pioneer of rocketry in America, who is known to have film-cooled the combustion-chamber walls of experimental rocket motors in the year 1929. (Cf. Ref. 1, p. 3).

liquid is one of the propellants, it is subsequently injected into the motor. (b) Prevent heat from entering the motor wall. This state is usually achieved by interposing a thin protective layer of liquid having a reasonably large heat of vaporization (frequently one of the propellants) between the combustion gases and the inner surface of the motor wall, the liquid evaporating into the heated gas stream. Disadvantages of the first solution are that not all propellants have physical and chemical properties suitable for this cooling method; because of the finite thickness of the motor wall, the temperature of the inner surface of the wall (determined by the heat-transfer rate, wall thickness, wall conductivity, and outer-wall surface temperature) may exceed the prescribed safe temperature even when a coolant is passed over the outer wall surface; and the pressure drop through the cooling passages (added to the chamber pressure and the pressure drop through the propellant injector orifices) may require an excessively heavy propellant supply system. The principal disadvantage inherent in the second solution is that the thrust produced by a film-cooled motor is usually less than that of a similar motor which is cooled by some other method and which has a propellant-flow rate equal to the combined propellant- and coolant-flow rates of the film-cooled motor. (An upper bound to this performance loss is given by the ratio of the coolant-flow rate to the combined propellant- and coolant-flow rates. For large rocket motors, this ratio is less than 0.01.) The manner in which these several disadvantages affect the cost and the performance of the missile should be considered when determining which solution to the cooling problem is to be employed.

The benefits of film cooling are most fully realized when the liquid film is attached to the surface without loss of unevaporated liquid to the proximate fluid stream, the attached liquid film is stable (i.e., no unevaporated liquid is lost to the proximate fluid stream as the result of disturbances on the film surface), and the evaporation rate is low.[a] It is therefore important to know how these three conditions may be obtained.

---

[a] If the given surface is the inner wall of a rocket motor, it is also desirable that the liquid be reactive with the combustion products, thereby acting, at least to some extent, as an injected propellant as well as a film coolant; that the liquid be one of the propellants, so that no special supply system is required for the coolant; and that an inexpensive non-critical, light-weight material (perhaps aluminum; cf. Ref. 2) be used in the construction of the combustion-chamber wall.

I-B: Previous Studies of Liquid-Film Attachment

Previous systematic studies of the liquid-film-attachment problem were limited to the experimental determination of the critical velocity of injection when a slot around the duct circumference is used (Cf. References 3, 4, and 5). The critical velocity of injection was defined as the maximum obtainable mean velocity of the liquid in the injection slot with no visible separation of the liquid film from the inner surface of the test section; it was found to depend upon the liquid density, liquid viscosity, duct configuration, gas-stream velocity, and injection-slot configuration but not upon gravity and the surface tension of the liquid. The authors of these papers asserted that the use of injection slots would provide more uniform liquid films and more easily controlled liquid-flow rates than could be obtained with other film-attachment methods. Remarks on these assertions will be made in Parts III and IV.

I-C: Previous Studies of Liquid-Film Stability

The stability of thin liquid wall films flowing under the influence of high-velocity turbulent gas streams has been investigated experimentally by Kinney and Abramson of the National Advisory Committee for Aeronautics (Cf. Reference 6) and to a limited extent by Greenberg of Purdue University (Cf. Reference 5).

Kinney and Abramson visually observed annular liquid flow with concurrent turbulent air flow in 2- and 4-inch-diameter horizontal transparent tubes. The experiments were conducted with air-mass velocities from 30.6 to 108 pounds per second per square foot, air temperatures of 80, 475, and 800°F, and gas-stream-diameter Reynolds numbers from 410,000 to 2,900,000. The liquid flows consisted of water, water-detergent solutions, and aqueous ethylene glycol solutions (which varied surface tension and liquid viscosity) at flow rates of 0.027 to 0.270 pound per second per foot of tube circumference (0.3 to 21 per cent of the air flows). The surface of the liquid film was observed to be relatively smooth at low liquid-flow rates and markedly disturbed at higher liquid-flow rates. The authors reported that the liquid flow per circumferential length at which marked liquid-flow disturbances initially occurred increased with increased liquid viscosity, increased slightly with decreased liquid surface tension, and did not vary appreciably with changes of air-mass velocity.

Kinney and Abramson presented a portion of their data in the form shown in Figure 1, where the heat-transfer results from a report by Kinney and Sloop (Cf. Reference 7) are included as well

as the research results reported in Reference 6. The curve is the dimensionless velocity correlation for adiabatic single-phase pipe flows which was given by Deissler (Cf. Reference 8); the abscissa is the dimensionless distance y*, defined by $y^* = \rho_o \sqrt{\tau_o/\rho_o}\,(y/\mu_o)$, and the ordinate is the dimensionless velocity u*, defined by $u^* = u/\sqrt{\tau_o/\rho_o}$, where τ is shearing stress, ρ is density, y is distance into the fluid stream measured perpendicularly to the duct wall, μ is dynamic viscosity, u is axial velocity, and the subscript o refers to the duct wall. The break in the curve of Figure 1 indicates approximately the transition from the laminar region to the turbulent region. The points which have been singled out on the curve correspond to the values of the dimensionless film thicknesses at which the liquid-film surface initially became rough; they were singled out in order to indicate the magnitude of the critical dimensionless film thickness relative to the dimensionless laminar sublayer thickness for single-phase pipe flows. Kinney and Abramson subscribed to the hypothesis, suggested earlier by Colburn and Carpenter (Cf. Reference 9), that an annular liquid film flowing under the influence of a high-velocity turbulent gas stream behaves as the wall layer with the same thickness and shearing stress in single-phase liquid flow and that it is essentially laminar when its thickness is less than the thickness of the laminar sublayer in the corresponding single-phase flow. Remarks on this hypothesis are included in Part IV-B.

Of the quantitative results for flows in transparent tubes which were presented by Kinney and Abramson, it is possible that

those depending upon values of fluid properties which vary appreciably with temperature changes (especially those depending upon values of liquid viscosities) may contain slight errors. The authors calculated fluid properties assuming the film temperature to be the same as that of the entering fluids (i.e., $80^{\circ}F$); actually, the film temperature was more nearly the wet-bulb temperature corresponding to the relative humidity of the gas stream (Cf., e.g. Equation (39) of this paper). Since the gas was virtually dry air (according to a personal communication from Kinney), this wet-bulb temperature was approximately $50^{\circ}F$, a temperature considerably lower than the $80^{\circ}F$ of the entering fluids.

Greenberg, in his MS thesis, included nine photographs of annular liquid flow with concurrent air flow in a horizontal Lucite tube. In the first of these photographs (Figure 23 of Reference 5) the surface of the liquid film appeared to be relatively smooth. The other eight photographs, taken at higher liquid-flow rates, indicated varying degrees of liquid-film surface disturbance. No correlation of the inception points of the marked disturbances was attempted by Greenberg in the thesis.

I-D: Previous Studies of Evaporation from Liquid Films

Of the several works published in recent years on evaporation from annular liquid wall films into heated turbulent gas streams, only the most comprehensive papers are reviewed here. These are the theoretical paper by L. Crocco (Cf. Reference 10) and the experimental paper by Kinney (Cf. Reference 11); both papers appeared in 1952.

Crocco extended Rannie's (Cf. Reference 12) approximate theory of porous-wall cooling for inert coolants to porous,[a] sweat, and film cooling for the case in which the coolant itself is reactive with the hot gas stream. The liquid film was assumed to be stable, and axial gradients were neglected in comparison with radial gradients. He divided the gas stream into two regions: a central turbulent core where the gases are not affected by the addition of mass at the boundary and a laminar sublayer adjacent to the boundary where all the effects of mass addition are confined. (The boundary referred to may be either a liquid-gas interface or a porous wall, the choice depending upon the type of cooling which is employed.) In the turbulent core, the Reynolds analogy was extended to read

$$\frac{\theta_\infty - \theta_\delta}{\dot{w}_\delta} = \frac{H_{t_\infty} - H_{t_\delta}}{\dot{q}_\delta} = \frac{u_\infty - u_\delta}{\tau_\delta} \qquad (1)$$

where θ is the oxidizer specific concentration (weight of oxidizer per unit total weight), $\dot{w}$ is oxidizer transfer per unit area and per unit time, H is enthalpy, $\dot{q}$ is heat transfer per unit area and per unit time,

---

[a] Crocco defined porous cooling as "cooling through a porous wall with a gas or a liquid vaporized before entering the wall" and sweat cooling as "cooling through a porous wall where the coolant is liquid throughout the wall."

the subscript ∞ refers to bulk properties or average velocity, the subscript s refers to the junction of the laminar sublayer and the turbulent core, and the subscript t refers to total (indicating that chemical energy, but not kinetic energy, of the fluid should be included). The thickness of the laminar sublayer in the gas stream δ was given by the relation

$$\frac{\rho_\infty \sqrt{\tau_o/\rho_\infty}\ \delta}{\bar{\mu}_M} = 5.6 \qquad (2)$$

where the subscript M refers to the mixture of gases, and a bar over the symbol for a fluid property indicates that the appropriate averaged quantity should be used. (Equation (2) was extended, in the absence of better information, from Prandtl's assumption for isothermal pipe flows.) Crocco treated the Schmidt and Prandtl numbers (equal, respectively, to $\mu/\rho D$ and $c_p \mu / k$, where D is molecular mass diffusivity, c_p is specific heat at constant pressure, and k is thermal conductivity) as invariants with respect to distance in the laminar sublayer. He further considered the combustion gases to be diffused as a whole, the driving potential for mass transfer to be specific concentration, and the reaction times of the mixtures to be short in comparison with other times involved. Remarks are made concerning Crocco's treatment of the turbulent core and assumption concerning the driving potential for mass transfer in Part V-A. The assumption of negligible axial gradients in comparison with radial gradients is discussed in Part V-B.

Crocco subsequently obtained a relation between the temperature of the boundary (either a liquid-gas interface or a porous wall) and the rate of mass addition at the boundary for given gas-

stream conditions and coolant properties. This relation permits the wall temperature to be determined for porous cooling when the rate of mass addition at the boundary is given, or the evaporation rate to be determined for sweat or film cooling if the liquid-film temperature is known. (Crocco assumed the liquid-film temperature to be equal to the boiling temperature of the liquid under the prevailing pressure. A general method for calculating the liquid-film temperature, based on a proposed extension of the wet-bulb-thermometer equation, is included in Part V-A.) Results of numerical calculations for gasoline and for water, both of which were evaporating into products of combustion of gasoline and oxygen, were presented.

Kinney reported on investigations of liquid-film cooling in 2- and 4-inch-diameter straight horizontal tubes having honed inner surfaces with air flows at temperatures from 800 to 2000°F and diameter Reynolds numbers from 220,000 to 1,100,000. The coolant was water which was injected at a single axial position on the tube at flow rates from 0.02 to 0.24 pound per second per foot of tube circumference (0.8 to 12 per cent of the air flow). Cooling effectiveness was determined by means of wall-temperature measurements. The results of the experiments were plotted on a single curve which relates the length of cooled surface with the coolant-flow rate when gas-stream parameters and fluid properties are specified.

In a comment (Cf. Reference 13) on Crocco's paper, Abramson compared the theoretical results of Crocco with the

experimental results reported by Kinney. The theory predicts a greater liquid-cooled length for all coolant-flow rates than were observed experimentally; only the large deviations at high coolant-flow rates (the result of film instability) were explained by Abramson.

I-E: Condensing Versus Evaporating Films

Since this study is presented with evaporating films uppermost in mind, comments on the applicability to condensing films of results obtained from studies of evaporating films are in order.

For the parameter ranges which were investigated, it was found that the film stability does not depend on mass-transfer rate. Hence, the results of the present film-stability investigation may be applied to evaporating and condensing films alike, provided, of course, that shearing stresses are large enough to make gravity forces negligible. Caution should be exercised, however, when applying the present results to cases in which the mass-transfer rates are much larger than those which have been investigated.

The treatment given the mass-transfer process in the present paper cannot be applied to general condensing films. For evaporating films of the type which were investigated, the heat transfer from the liquid film to the duct wall is negligible compared with the heat transfer to the liquid film from the gas stream (gas-stream temperature and velocity gradients are relatively large); for general condensing films, the heat transfer from the liquid film to the duct wall is large compared with the heat transfer to the liquid film from the gas stream (gas-stream temperature and velocity gradients are relatively small).

I-F: Purpose and Scope of Present Study

As indicated earlier (Cf. Part I-A), the benefits of film cooling are most fully realized when the liquid is attached to the solid surface without entrainment of liquid droplets by the proximate gas stream, the attached liquid film is stable, and the evaporation rate is low. Little basic information was available in 1950 regarding the prerequisites for these conditions. Consequently, a study was initiated during that year for the purpose of obtaining a basic understanding of thin liquid wall films flowing under the influence of high-velocity turbulent gas streams by investigating the attachment of liquid films to solid surfaces in the presence of high-velocity gas streams, the conditions which are sufficient for stability of liquid wall films flowing under the influence of high-velocity turbulent gas streams, and the rate of evaporation from a stable liquid wall film into a heated turbulent gas stream.

The essential results of the investigation can be summarized as follows: (a) The attachment of liquid films to solid surfaces by using radial-hole injectors in conjunction with the effects of high-velocity gas streams is concluded to be effective over a useful range of operating conditions. (b) An annular liquid film flowing under the influence of a high-velocity turbulent gas stream is found to differ from the wall layer with the same thickness and shearing stress in single-phase liquid flow in that the dimensionless thickness of a liquid film corresponding to the inception point of unstable flow is a function of fluid properties, whereas the dimensionless

thickness of the laminar sublayer in single-phase liquid flow has a constant value. (c) The liquid-film surface temperature is found experimentally to agree with surface temperatures calculated from the wet-bulb-thermometer equation extended to the case when large temperature and partial-pressure gradients occur. (d) A method for treating the effects of mass addition on transport phenomena in the turbulent core as well as in the laminar sublayer of a gas stream flowing proximate to an evaporating liquid film is proposed.

II. EXPERIMENTAL EQUIPMENT

II-A: Equipment for Film-Attachment Studies

The flow diagram for the equipment used in the film-attachment studies (Cf. Reference 14) is presented in Figure 2. The equipment consisted essentially of an air-supply system, a liquid-supply system, a Lucite test section, and appropriate controlling and measuring devices.

The air was obtained from the standard air-supply system in general use at the Jet Propulsion Laboratory; its flow rate was measured with the aid of a sharp-edge orifice which had been designed according to ISA specifications, a 30-inch mercury manometer, a Bourdon-type pressure gage, and an iron-constantan thermocouple. After being passed through the measuring orifice, the air was conducted through the Lucite test section (located 46 diameters downstream from the measuring orifice) and exhausted to the atmosphere through a manually operated gate valve (located 16 diameters downstream from the test section). The magnitude of the static air pressure in the test section, which was controlled by the gate valve, was measured with a Bourdon-type pressure gage, and the air temperature in the test section was measured with the aid of an iron-constantan thermocouple.

The liquid used in the tests was stored in a metal tank pressurized by nitrogen gas from a commercial compressed-nitrogen bottle. From the storage tank the liquid was conducted through a rotameter, a manually operated needle valve, a screen

filter and finally into the test section through one of the four available injector openings. The liquid temperature was measured at a point several inches upstream from the injector with the aid of an iron-constantan thermocouple; electric potentials from the thermocouples were measured with the aid of a hand-balanced potentiometer.

The Lucite test section was fabricated from commercially available stock having a 3-inch inside diameter and a 1/4-inch wall thickness. Lucite was selected because of its transparency and good machining properties. Four radial holes, ranging from 1/16 to 5/32 inch in diameter, were drilled at 90° intervals around the periphery of the test section. During any given test, liquid was injected through only one of these holes; the other holes were utilized as static-pressure taps and thermocouple sites.

A total-pressure probe attached to a manually operated micrometer screw was used for the purpose of investigating the velocity profile of the air flowing in the test section. Tests were conducted only after the velocity profile was found to be symmetric with respect to the center line of the duct.

II-B: Equipment for Film-Stability and Evaporation-Rate Studies

The flow diagram for the equipment used in the film-stability and evaporation-rate studies is presented in Figure 3. The equipment consisted essentially of a gas-supply system, a liquid-supply system, several interchangeable test sections, and appropriate controlling and measuring devices.

The gas was in general produced by burning fuel (Union Oil Company's No. 1 thinner) and air in a modified turbojet combustion can. The fuel flowed into the burner from a nitrogen-pressurized storage tank; its flow rate was measured with the aid of Bourdon-type pressure gages and a calibrated injection nozzle. The air was obtained from the standard air-supply system in general use at the Jet Propulsion Laboratory; its flow rate was measured with the aid of a sharp-edge orifice which had been designed according to ISA specifications, a 50-inch mercury manometer, a Bourdon-type pressure gage, and a chromel-alumel thermocouple. The products of combustion were mixed and subsequently calmed in an insulated settling chamber having a cross-sectional area eighteen times that of the approach duct. After passing through the settling chamber, the combustion products flowed through 27 diameters of insulated, straight, constant-diameter approach duct and then into the test section. The total gas temperature in the settling chamber was measured with the aid of a shielded chromel-alumel thermocouple; the magnitude of the static pressure in the approach section immediately upstream from the injector was measured with a Bourdon-type pressure gage; and the pressure drop in the test section was measured with the aid of a 50-inch water manometer.

Water (procured directly from the Laboratory water supply pipe at approximately 100 psig) and aqueous sucrose solutions (produced by mixing tap water and reagent sucrose and stored in a nitrogen-pressurized supply tank) constituted the liquids in the film-stability tests; water was the only liquid used in the evaporation-rate tests. After leaving the Laboratory water-supply line (or the supply tank, as the case may be), the liquid flowed (in the sequence named) through one of two manually operated needle valves, one of two rotameters, a filter, the coolant-injector plenum chamber (Cf. Figure 4), twenty-four (twelve, for one group of tests) 0.011-inch-square passages (characterized by relatively high flow resistances and serving to nullify gravity effects in the plenum chamber), and corresponding equally spaced, 1/16-inch-diameter, radial-injection holes. The liquid was attached to the inner wall of the test section by the action of the high-velocity gas stream. For tests employing unheated gases, the film temperature was assumed to be equal to the wet-bulb temperature in the case of a water film and the temperature (measured) of the exhausted liquid in the case of a film of aqueous sucrose solution; for tests employing heated gases, the film temperature was calculated using Equation (39) of this paper.

For use in tests employing heated gases, a test section was fabricated from a 5-foot length of 347 stainless-steel tubing having a 0.063-inch wall and a 3-inch outside diameter. The inside diameter of the tube was honed to 2.90 inches (leaving a wall thickness of 0.050 inch), and 120 thermocouples were spot-welded to the outside of the tube, one every inch (measured axially) at the 12 o'clock

position and one every 3 inches at the 3, 6, and 9 o'clock positions. For use in tests employing gases at ambient temperature, several lengths of Lucite tubing having a 3-inch inside diameter and a 0.25-inch wall were procured.

The electric potentials from the thermocouples which were used in order to facilitate the measurement of the gas temperature and eight of the test-section-wall temperatures were recorded on a 12-point, 50-millivolt-range Brown recorder located in the control room. The remaining 112 thermocouples were connected in turn to a continuously recording, single-channel potentiometer located at the Jet Propulsion Laboratory central recording room by means of a 25-point, 10-level, telephone-type automatic electric stepping switch capable of scanning the 112 thermocouples in less than 2 minutes.

III. LIQUID-FILM ATTACHMENT WITH RADIAL INJECTOR HOLES AND A HIGH-VELOCITY GAS STREAM

III-A: Experimental Results

An experimental study was conducted in order to determine the critical velocity of injection for attachment of a liquid film to the inside of a circular duct when radial injector holes and effects of a high-velocity gas stream are used (Cf. Reference 14). The critical velocity of injection was defined as the maximum mean velocity of the liquid in the injector orifices obtained with no visible separation of the coolant film from the inner surface of the test section.

Liquid viscosities from 1.59×10^{-5} to 10.69×10^{-5} pound second per square foot, liquid densities from 1.94 to 3.02 slugs per cubic foot, and liquid vapor pressures from 0.15 to 3.85 pounds per square inch absolute were secured by using water, aqueous zinc chloride solutions, aqueous sucrose solutions, and carbon tetrachloride. Test-section air densities from 2.26 to 9.58×10^{-3} slug per cubic foot were provided by a gate valve at the discharge end of the air duct; no other appreciable gas-property variations were realized. Injector-orifice diameters varying from 1/16 to 5/32 inch were achieved by using different injectors; no gas-duct diameter variations were realized. (Cf. Part II-A for description of equipment.)

For each test point, the air-supply system was operated at the desired output until a stable air-flow rate was obtained. When this condition was realized, the liquid-flow rate was increased slowly from the no-flow value to a value when the critical velocity of injection was reached. At that instant the air-flow rate, the injected-liquid-flow rate, and the appropriate temperatures and pressures

were recorded. The data taken at the critical injection velocity are given in Table I of Reference 14.

Incidental to the obtainment of attachment data, the circumferential spread of the liquid film corresponding to liquid flows at twenty-one different critical injection velocities was measured at a point arbitrarily located 1.25 inches downstream from the injection point. The spread appeared to be chiefly a function of the liquid-flow rate; i.e., the fluid properties, the air velocity, and the injector-hole diameter apparently had a minor effect on the spread for the range of fluid properties and air velocities tested. Typical values of the spread were 0.75 inch for 1.5×10^{-4} slug per second and 1.50 inches for 6.0×10^{-4} slug per second of liquid flow. Since the spread would vanish as the liquid-flow rate approached zero, the data would seem to indicate that the circumferential spread is proportional to the square root of the liquid-flow rate.

III-B: Discussion of Data

Since no theoretical analysis of the film-attachment problem has been made, the data were plotted in dimensionless form (Cf. Figure 5); the abscissa is a function of gas-stream Reynolds number Re_G, liquid-stream Reynolds number Re_{Li}, and a modified cavitation parameter Ca_{Li}, and the ordinate is the ratio of the gas- and liquid-stream momenta $\rho_\infty u_\infty^2/\rho_{Li}V^2$. Here Re is Reynolds number based on diameter, Ca is a modified cavitation parameter defined by $Ca = \rho_{Li}V^2/(p-p_V)$, p is pressure, V is liquid velocity averaged over the cross-sectional area of the injection orifices, and the subscripts G, Li, and V refer to gas, liquid in the injector orifice, and vapor, respectively. The exponents of the dimensionless parameters were determined from crossplots on log-log paper of liquid- and gas-stream parameters for a constant value of the momentum ratio. (The line drawn in Figure 5 has a scope of 0.8.) The dimensionless parameters used are speculative to the extent that the gas viscosity and test-section diameter were held constant and the vapor pressure of the liquid was varied over only a small range during the tests; e.g., with available data it was not possible to discern whether the significant gas-stream Reynolds number is that (based on gas velocity u_∞) which describes the gas stream in general or that (based on friction velocity $\sqrt{\tau_o/\rho_o}$) which describes only the gas flow near the duct wall.

Figure 5 indicates that efficient film attachment is obtained when liquid-stream inertia forces are small, gas-stream inertia forces are large, liquid- and gas-stream viscous forces are large, the liquid-stream vapor pressure is small, and the gas-stream

static pressure is large. These requirements for efficient film attachment are in general agreement with those which one would intuitively expect.

It is concluded that effective film attachment may be obtained with simple radial-hole injectors in the presence of a high-velocity gas stream over a useful range of operating conditions so that the study of more complex means of injection (such as porous walls and circumferential slots) and of insuring film attachment is probably not required. It is furthermore concluded that the critical velocity of injection is a definite function of certain parameters of the system; thus it is possible to predict beforehand whether a given film-coolant stream will attach to the wall or will continue on into the gas stream.

Figure 5 should be a useful guide in the design of film-cooling systems for turbulent flat-plate flows as well as for turbulent duct flows. Until further information is obtained, it is suggested that twice the local boundary-layer thickness be taken to be the characteristic gas-stream dimension in the case of flat-plate flows; this dimension corresponds to the duct diameter which was used in the case of pipe flows. Obviously, caution should be exercised when extending the presented results to parameter values outside the investigated range.

Since the calculation of streamlines for viscous fluid flows around sharp corners is an extremely difficult talk, it seems unlikely that an analytical study of the film-attachment problem would be a rewarding undertaking at the present time. Experimental

methods, on the other hand, have already been successfully used for the determination of the relative importance of several parameters involved in the film-attachment process. Therefore, if it should be deemed necessary to obtain further information concerning liquid-film attachment, it is suggested that (at the present time) experimental studies might be most profitable.

As stated before, the dimensionless parameters which were used in the presentation of the data (Cf. Figure 5) are speculative due to the restriction on the variation of test parameters. (These limitations were imposed upon the study by the equipment and liquids which were used.) For more complete information it will be necessary to do experiments covering wide ranges of gas viscosities, test-section diameters, and vapor pressures.

As mentioned in Part I, it is possible that film cooling will be used for (among other things) the protection of the external surfaces of guided missiles and the internal surfaces of rocket-motor nozzles. If simple film-coolant injector holes are to be located on these surfaces, it would be necessary to study the film-attachment phenomena at supersonic gas velocities and for various surface geometries.

IV. STABILITY OF LIQUID FILMS FLOWING UNDER THE INFLUENCE OF TURBULENT GAS STREAMS

IV-A: Experimental Results

The dividing line between the areas of stable and unstable flow of annular liquid wall films in the presence of high-velocity turbulent gas flow in a duct has been detected both indirectly, by inspection of mass-transfer data, and directly, by examination of the liquid film itself (Cf. Reference 6). During the present investigation, the first method was used when heated gases were employed, and the second method was used when gases at room temperature were employed.

Data concerning the rate of mass transfer into a turbulent heated gas stream from a liquid wall film (averaged over the length of the film) were obtained for specified operating conditions by operating the test apparatus at the desired gas-flow rate, gas temperature, and liquid-flow rate until steady-state conditions were attained and then by recording (together with other pertinent data) the electric potentials created within thermocouples which were spot-welded to the exterior of the metal test duct. The axial position along the duct at which the wall temperature varied rapidly from a value below that of the boiling temperature of the liquid to a value approaching that of the hot gas stream was assumed to coincide with the axial position along the duct corresponding to the end of the protective liquid film. Tests were conducted for gas-stream-diameter Reynolds numbers from 105,000 to 433,000, gas-stream temperature from 1103 to 2239°R, water-flow rates from 0.012 to 0.20 pound per second per foot of tube circumference, and

ambient pressures. (Cf. Part II-B for a description of the equipment which was used.)

Results of the mass-transfer tests (Cf. Table I) are presented in raw form in Figures 6 and 7, where the protected-surface area is plotted on the abscissa and the corresponding water-flow rate is plotted on the ordinate. (Note that the mass-transfer rate, averaged over the film length, may be readily calculated for a given set of operating conditions by dividing the ordinate by the abscissa for the appropriate test conditions.) Figures 6 and 7, respectively, indicate the effect of gas-flow rate and gas-stream temperature on the mass-transfer rate. The points at which the slopes of the curves drawn through the data change abruptly were located with the aid of auxiliary plots of test-section pressure drop (Cf. Table I) vs area of protected surface and test-section pressure drop vs liquid-flow rate. Curves with abruptly changing slopes were also drawn through the points on the auxiliary plots, and it was assumed that the slopes of the three curves (liquid-flow rate vs protected-surface area, pressure drop vs protected-surface area, and pressure drop vs liquid-flow rate) changed abruptly at the same value of protected-surface area or, as the case may be, liquid-flow rate.

For the direct study of the character of liquid wall films, a Lucite test section was installed in the test apparatus; study mediums included high-speed motion pictures, spark photographs, and visual observations aided by stroboscopic lighting.

High-speed motion pictures were taken for gas-stream-diameter Reynolds numbers from 239,000 to 664,000, water-flow

rates from 0.031 to 0.12 pound per second per foot of tube circumference, ambient pressures, and ambient temperatures. The pictures make manifest the following facts for the range of variables investigated:

1. Small disturbances with wavelengths of the order of 10 film thicknesses are present on the surface of the liquid film for all liquid-flow rates.
2. The scale of the small disturbances decreases as the diameter Reynolds number of the gas stream increases; the scale does not vary appreciably, however, when the liquid-flow rate is changed.
3. For liquid-flow rates larger than some critical value, long-wavelength disturbances appear on the surface of the film.
4. The inception point of the long-wavelength disturbances is independent of the gas-stream Reynolds number.
5. Liquid droplets are entrained by the gas stream from the crests (regions where relatively large quantities of liquid are collected) of the long-wavelength disturbances.

Spark photographs were taken for gas-stream-diameter Reynolds numbers from 310,000 to 560,000, water-flow rates from 0.021 to 0.097 pound per second per foot of tube circumference, ambient pressures, and ambient temperatures. They confirmed items 1 through 4 of the preceding paragraph and presented additional detailed qualitative information concerning the structure of the disturbances. Figure 8 indicates the effect of varying the liquid-flow

rate for given gas-stream parameters; Figure 9 shows the effect of varying the gas-flow rate for given liquid-film parameters. (Photographs of the type presented in Figures 8 and 9, incidentally, do not reveal any film non-uniformities which may be attributed to the fact that the film was injected through discrete holes. This state of affairs is good; circumferential film non-uniformities are undesirable in most film-cooling applications.)

Visual observations aided by stroboscopic lighting were made for gas-stream-diameter Reynolds numbers from 307,000 to 595,000, test-section pressures from 14.1 to 28.9 psia, viscosity ratios (μ_{M_o}/μ_{Lf}) from 0.0052 to 0.0140 (obtained by using water and aqueous sucrose solutions), and ambient temperatures. For given gas-stream conditions and given fluid properties, the liquid-flow rate corresponding to the observed inception point of unstable liquid-film flow was determined in nine separate trials. The median of the flow rates corresponding to the nine trials was accepted for comparison with data obtained by other study mediums.

Quantitative results of the tests at ambient temperatures are presented in Table II, where the median of the results for water-air flows given in Reference 6 is included as well as present data.

IV-B: Discussion of Data

Flows with Heated Gases. Results of studies on film attachment (Cf. Part III) indicate that if, for given gas-stream parameters, the product $(\rho_{Li}V^2)^{1.25}(Re_{Li}Ca_{Li})^{0.5}$ is greater than some critical value, then a portion of the injected liquid will be entrained by the gas stream without serving to protect the test-section wall. Hence, the possibility of inefficient film attachment at high liquid-flow rates causing (for a given set of gas-stream conditions) the increased averaged mass-transfer rate from a liquid film when the liquid-flow rate exceeds some particular value (as evidenced by the increase of the slope of any given curve in Figures 6 and 7) should be investigated. Such an investigation reveals that, if the straight line drawn in Figure 5 can be extended as a straight line to higher gas-stream parameters, then the critical velocity of injection was exceeded in only five of the tests for which data are given. (These five tests are represented by the filled-in circles in Figure 6.) More specifically, Figure 5 indicates that the critical velocity of injection for the curve corresponding to tests 107 through 118 should occur at a liquid-flow rate of 0.10 pound per second. Hence, the abrupt change in the slope of the curve for tests 107 through 118 which occurs at approximately 0.10 pound per second of liquid flow is interpreted to be the result of inefficient film attachment for flow rates higher than 0.10 pound per second. The critical injection velocity was exceeded in tests 107 through 118 and not in tests 31 through 44 because for tests 107 through 118 alternate passages in the injector (i.e., twelve passages) were closed, whereas in the other tests all twenty-four passages were utilized for liquid injection.

The other abrupt changes in the slopes of the curves of Figures 6 and 7 (one abrupt change for each curve) are interpreted to mean that two different types of flow are encountered in film-cooling applications. One type of flow, found at relatively low liquid-flow rates, apparently leads to low mass-transfer rates, whereas the other type of flow, found at relatively high liquid-flow rates, apparently leads to high mass-transfer rates. Obviously, the latter type of flow is to be avoided if efficient coolant usage is desired.

The fact that the curves of test-section pressure drop vs liquid-flow rate (or vs protected-surface area) possess abrupt changes in slope which are related to film-attachment efficiency and film stability can be accounted for if one examines the equations of steady one-dimensional gas flow as developed by Shapiro and Hawthorne (Cf. Reference 15). For further discussion of this topic, see Appendix A.

Inspection of available data (including those presented by Kinney in Figure 4 of Reference 11) for the flow of heated air over a thin water film reveals that data corresponding to the inception point of unstable liquid-film flows (flows which are accompanied by high mass-transfer rates) may be presented in dimensionless form (Cf. Figure 10) by plotting the dimensionless film thickness corresponding to the inception point of unstable liquid-film flows as a function of the ratio of the gas-vapor-mixture viscosity to the liquid viscosity; the dimensionless film thickness is defined by $\eta^* = \rho_{Lf}\sqrt{\tau_i/\rho_{Lf}}\,(\eta/\mu_{Lf})$ and (assuming a linear velocity profile to exist in the liquid film) is calculated from $\eta^* = \sqrt{2\Gamma/\mu_{Lf}}$

(Cf. Table III), Γ is liquid flow per unit time and per unit length of tube circumference, η is average film thickness, the subscript Lf refers to the liquid in the film, and the viscosities are evaluated at the liquid-film surface temperature. The film temperatures were calculated (Cf. Table III and Figure 11) using Equation (39), and the mixture viscosities were calculated using the procedure suggested by Bromley and Wilke (Cf. Reference 16).

Since the liquid viscosity appears in both the abscissa and the ordinate of Figure 10 and the gas-vapor-mixture viscosity did not vary appreciably for the tests, it is interesting to replot the data after dividing the ordinate by the viscosity ratio (Cf. Figure 12). Further comments on Figures 10 and 12 are withheld until later in the discussion.

Flows with Unheated Gases. Data for gas flows at ambient temperatures (Cf. Table II) have been added to Figures 10 and 12; the film temperature was assumed to be equal to the wet-bulb temperature in the case of a water film and to the temperature (measured) of the exhausted liquid in the case of a film of aqueous sucrose solution.

The data presented in Figures 10 and 12 are for gas-stream-diameter Reynolds numbers from 105,000 to 2,900,000, duct diameters from 2 to 4 inches, test-section pressures from 14.1 to 28.9 psia, temperature ratios T_∞ / T_o from 1.0 to 3.5, and mass-flow ratios $\dot{m}_o / \rho_\infty u_\infty$ from zero to 0.0015 (where T is temperature and $\dot{m}$ is mass transfer per unit area and per unit time). Since the viscosity ratio μ_{M_o} / μ_{Lf} did not vary monotonically with any of these

parameters, the curves presented may be taken to be general curves which are valid for liquid-gas combinations other than those investigated (provided, of course, that the several parameter values do not vary too greatly from the ranges investigated).

The hypothesis that an annular liquid film flowing under the influence of a high-velocity gas stream behaves as a part of a single-phase boundary layer is now seen to be incorrect. Whereas the laminar sublayer thickness in a single-phase boundary layer is completely defined by the dimensionless thickness y*, Figure 10 indicates that the maximum allowable thickness of a stable liquid wall film flowing under the influence of a high-velocity gas stream depends upon both the dimensionless thickness η^* and the viscosity ratio μ_{M_o}/μ_{Lf}. The basis for this observed dissimilarity has not been established; it is suspected, however, that the velocity profile as influenced by the viscosity discontinuity at the liquid-gas interface has an appreciable effect on the stability of the liquid wall film (Cf. Figure 13 for a sketch of a velocity profile typical of that encountered in the case of a stable liquid wall film flowing under the influence of a turbulent gas stream).

Although dimensionless parameters (e.g., the ratio η/δ) other than those used in Figures 10 and 12 have been examined, only those used in Figures 10 and 12 were found to be satisfactory for data presentation.

Summarizing, examinations of data concerning mass transfer from liquid wall films, inspections of high-speed motion pictures and spark photographs of liquid wall films, and visual observations of liquid wall films led to the conclusion that the presence of unstable

long-wavelength disturbances on a liquid-film surface was accompanied by relatively high mass-transfer rates (due, at least in part, to the loss of liquid droplets from the unstable film surface to the gas stream); hence, the unstable long-wavelength disturbances are to be avoided when designing for an efficient film-cooling system. All available data corresponding to the inception point of instability for liquid wall films flowing under the influence of high-velocity gas streams are presented in dimensionless form by plotting the dimensionless film thickness corresponding to the inception point of instability as a function of the ratio of the gas-vapor-mixture viscosity to the liquid viscosity, where the viscosities were evaluated at the liquid-film surface temperature.

The dimensionless parameters which were used in the presentation of the data obtained at the inception point of film instability (Cf. Figures 10 and 12) are speculative inasmuch as the liquid density ρ_{Lf} and gas viscosity μ_{M_o} were not varied appreciably during the tests. Experiments with various liquid densities and various gas viscosities are required for the complete confirmation of the dimensionless parameters used in Figures 10 and 12.

Since the small disturbances which have been observed on the surface of a liquid film flowing under the influence of a turbulent gas stream appear to be related to the gas-stream turbulence, a complete analytical investigation of their origin would be difficult. However, much useful information could perhaps be obtained from an analysis of the stability of Couette flow with two layers of fluid of different densities and viscosities. Such a flow might be stable

to small oscillations for all Reynolds numbers, but the wavelengths and velocities of the least-damped oscillations are possibly related closely to the small disturbances observed on the surface of a liquid film. The fact that the wavelength of the small surface disturbances has been observed to be approximately 10 film thicknesses makes the suggested analysis appear promising; a typical result of stability analyses is that the least-damped oscillations have a wavelength of the order of ten times the characteristic length of the flow field.

Previous analytical studies of polygonal velocity profiles in viscous fluids by Tietjens (Cf. Reference 17) and Wuest (Cf. Reference 18) provide useful background material for the analysis suggested. Tietjens examined broken linear velocity profiles for flows of homogeneous fluids near solid boundaries for the purpose of determining the origin of turbulence in fluid flows. He considered viscosity to affect small disturbances only in a thin layer close to the solid boundary and specifically neglected viscous effects in the neighborhood of the plane where the propagation velocity of the disturbance equals the velocity of the mean flow; he obtained no lower limit for unstable flows. Wuest studied several velocity profiles (including linear velocity profiles) for flows of gas streams of infinite height over liquid streams of infinite depth for the purpose of determining the origin of wave motion at such a gas-liquid interface. He considered viscous effects on small disturbances throughout the entire flow field; he presented conditions for neutral stability of gravity and capillary waves for the several velocity profiles investigated.

The present investigator has carried through a preliminary analysis (unpublished) for the case of a gas stream of infinite height flowing rapidly over a thin liquid film flowing slowly along a solid boundary for the purpose of determining the origin of wave motion at a gas-liquid interface when gravity and capillary forces are nullified by high shearing stresses. The main-stream velocity was assumed to be constant in the gas stream and in the liquid film (giving a velocity discontinuity at the liquid-gas interface), but viscous effects on small disturbances were considered throughout the entire flow field. The only neutral stability which was found occurred for disturbances having a propagation velocity equal to the main-stream velocity of the liquid; no effects of liquid-film Reynolds number on the stability of infinitesimal disturbances were determined.

The stability analyses mentioned in the preceding several paragraphs might possibly lead to useful information concerning the origin of the small disturbances observed on the surface of a liquid film flowing under the influence of a turbulent gas stream; however, these analyses would most likely not lead directly to a determination of the origin of the long-wavelength disturbances which are characterized by entrainment of liquid droplets by the gas stream. It is possible that the origin of these long-wavelength disturbances is related to an interaction of the small finite-amplitude disturbances with the gas stream which results in destabilizing axial shearing-stress gradients.

V. EVAPORATION FROM STABLE LIQUID WALL FILMS INTO HEATED TURBULENT GAS STREAMS

V-A: Theoretical Analysis

A theoretical analysis of the mass-transfer process from a stable annular liquid wall film flowing under the influence of a fully developed turbulent heated gas stream in a duct is presented. The purpose is to show the relative importance of the several parameters which affect the evaporation rate and to determine the magnitude of the evaporation rate for given fluid properties and gas-stream parameters. It is believed that the analysis presented here differs from previous analyses in that the effects of mass addition on transport phenomena are given consideration in the turbulent core as well as in the laminar sublayer of the gas stream and that the surface temperature of the liquid film is calculated instead of estimated. Although the case in which the coolant itself is reactive with the hot gas stream is not explicitly analyzed here, the results obtained may be extended in a manner analogous to that employed by Crocco to extend Rannie's work.

Assumptions. In order to facilitate computations (and still obtain useful results), a model will be considered which has the following characteristics:

1. Variations with respect to time may be neglected.
2. The effects of body forces may be neglected in comparison with the effects of viscous and inertia forces.
3. Work done by viscous and pressure forces may be neglected in comparison with heat transferred because of temperature gradients.

4. Mass transfer due to temperature gradient may be neglected in comparison with mass transfer due to partial-pressure gradient.
5. The liquid-film surface velocity may be neglected in comparison with the average gas velocity.
6. The gas stream may be divided into two regions: a center core in which the fluid flow is predominantly turbulent and a laminar sublayer (adjacent to the liquid film) in which the fluid flow is predominantly laminar. (Comparisons of heat-transfer rates obtained for turbulent pipe flows with heat-transfer rates predicted by the Prandtl-Taylor equation justify such a division into two regions when the Prandtl and Schmidt numbers do not vary from unity by more than a factor of 2. Most gases satisfy this restriction.)
7. Axial variations in the gas stream are small compared with radial variations, and the laminar sublayer thickness of the gas stream is small compared with the pipe diameter. These features permit the assumption that transfer processes in the laminar sublayer are one-dimensional.
8. The heat which is transferred to the liquid film from the hot gas by convection and conduction is equal to that required for vaporization of the liquid. (This characteristic is attained if all liquid which leaves

the film is in the vaporized form, i.e., the film is stable, and if the net heat which is transferred to the liquid film by radiation is equal to the heat which is transferred from the liquid film to the duct wall plus the heat which is required to warm the liquid from the injection temperature to the evaporation temperature. In many cases, these three heat quantities are negligible in comparison with the heat required for vaporization of the liquid.)

9. The eddy heat diffusivity, eddy mass diffusivity, and eddy viscosity are equal in magnitude.
10. Mass diffusion in the laminar sublayer may be treated as a binary process even when more than two molecular species are present. Such a treatment is nearly correct unless the gas stream contains large concentrations of species having widely different molecular weights, e.g., large quantities of hydrogen and carbon dioxide. (This simplifying assumption is not necessary for the turbulent core since the mass diffusion in the turbulent core is the result of macroscopic mixing rather than molecular processes.)

Solution of the Problem. Steps in the solution of the problem will include (a) the derivation of heat-, mass-, and momentum-transfer relations in the laminar sublayer, (b) the postulate of an extension of the Reynolds analogy to heat, mass, and momentum

transfer in the turbulent core of two-component turbulent pipe flow with unidirectional radial diffusion, and (c) the combination of results of a and b in order to obtain the desired relations between evaporation rate, fluid properties, and gas-stream parameters, applicable to stable annular liquid wall films flowing under the influence of fully developed heated turbulent gas streams when entrance effects are negligible.

First, consider the laminar sublayer. Since evaporated coolant is not being stored in the laminar sublayer, it follows immediately that $\dot{m}$ is not a function of y in the laminar sublayer, where y is distance into the gas stream from the liquid-gas interface measured perpendicularly to the film surface. Furthermore, assumption 8 implies that heat transferred by conduction across the liquid-gas interface is equal to $-\dot{m}_o \Delta H$, where ΔH is coolant latent heat of vaporization. Hence, one may write the heat, mass, and force balances for the laminar sublayer in the forms

$$-k_M \, dT/dy + \dot{m}_o \bar{c}_{p_V} T = -\dot{m}_o \Delta H + \dot{m}_o \bar{c}_{p_V} T_o \tag{3}$$

$$\frac{pD}{R_V T} \frac{d}{dy} \ln (p - p_V) = \dot{m}_o \tag{4}$$

$$-\mu_M \frac{du}{dy} + \dot{m}_o u = -\tau_o \tag{5}$$

where R is the gas constant. (Note that the driving potential for mass transfer is properly taken to be partial pressure instead of specific concentration; this treatment is essential when the

molecular weight of the coolant differs greatly from that of the hot gas.) Rearrangement of Equations (3), (4), and (5) and integration between the limits o and δ yield the relations

$$\frac{\bar{c}_{p_M}}{\bar{c}_{p_V}} \ln\left(\frac{\Delta H + \bar{c}_{p_V}(T_\delta - T_o)}{\Delta H}\right) = \bar{P}r_M \frac{\dot{m}_o \delta'}{\mu_{M_o}} \tag{6}$$

$$\frac{\bar{R}_M}{R_V} \ln\left(\frac{p - p_{V_\delta}}{p - p_{V_o}}\right) = \bar{S}c_M \frac{\dot{m}_o \delta'}{\mu_{M_o}} \tag{7}$$

$$\ln\left(\frac{\gamma_o + \dot{m}_o u_\delta}{\gamma_o}\right) = \frac{\dot{m}_o \delta'}{\mu_{M_o}} \tag{8}$$

where Pr is Prandtl number, Sc is Schmidt number, and

$$\delta' = \int_o^\delta \frac{\mu_{M_o}}{\mu_M} dy \tag{9}$$

Equations (6) through (9) completely describe the relationships between conditions at the liquid-gas interface and conditions at the junction of the laminar sublayer with the turbulent core.

Second, consider the turbulent core. A logical extension of the Reynolds analogy (Cf. Reference 19 for Reynolds' statement of the hypothesis) to heat, mass, and momentum transfer in the turbulent core of non-reacting, two-component pipe flows with unidirectional radial diffusion must specify that the rate of radial momentum transport at any point of the flow field under consideration bears the same relation to the gradients which produce momentum flow as the energy-transfer rate bears to the gradients which produce energy

flow and as the mass-transfer rate bears to the gradient which produces mass flow. Whether heat and momentum carried in the radial direction by the diffusing vapor should or should not be included in an analogy of this type is not immediately apparent. However, since velocity, temperature, and partial-pressure profiles are joined most smoothly at the junction of the laminar sublayer and turbulent core when heat and momentum carried by the diffusing vapor are considered in the turbulent core as well as in the laminar sublayer, it seems reasonable that the effects of mass diffusion on heat and momentum transfer in the turbulent core should be included in the proposed Reynolds analogy extension. (Obviously, as was the case for Reynolds' original hypothesis, the merits of this suggestion can be conclusively established only by experimental means.) Following this suggestion, the extension of the Reynolds analogy to heat, mass, and momentum transfer in the turbulent core of two-component turbulent pipe flows with unidirectional radial diffusion is postulated to be

$$\frac{\dot{m}_s}{\frac{p}{R_v T}\frac{d}{dy}\ln(p-p_v)} = \frac{\dot{q}_s + c_{p_v} T_s \dot{m}_s}{-\rho_m c_{p_m}\frac{dT}{dy} + c_{p_v} T \frac{p}{R_v T}\frac{d}{dy}\ln(p-p_v)} \tag{10}$$

$$= \frac{-\tau_s + u_s \dot{m}_s}{-\rho_m \frac{du}{dy} + u \frac{p}{R_v T}\frac{d}{dy}\ln(p-p_v)}$$

(Cf. Appendix B for the identification of $\dot{m}$, $\dot{q}$, and τ with time averages of turbulent fluctuations.) Equations (10) differ from Crocco's extension of the Reynolds analogy in that consideration has been given the effects of mass addition on transport phenomena in the turbulent core and that the driving potential for mass transfer is taken to

be partial pressure. For given boundary conditions, Equations (10) completely prescribe relations between heat, mass, and momentum transfer in the turbulent core of the model being considered.

The combination of the results of the previous two paragraphs will now provide the desired relations between evaporation rate, fluid properties, and gas-stream parameters. Noting that at $y = \delta$ Equations (3), (4), and (5) read

$$\dot{q}_\delta = - \dot{m}_o \Delta H - \dot{m}_o \bar{c}_{p_V} (T_\delta - T_o) \tag{11}$$

$$\dot{m}_\delta = \dot{m}_o \tag{12}$$

$$\tau_\delta = \tau_o + \dot{m}_o u_\delta \tag{13}$$

one may rearrange Equations (10) to read

$$\frac{R_M}{R_V} d \ln (p - p_V) = \frac{c_{p_M}}{\bar{c}_{p_V}} d \ln [\Delta H + \bar{c}_{p_V} (T - T_o)] = d \ln (\tau_o + \dot{m}_o u) \tag{14}$$

which, when integrated between $y = \delta$ and a point far into the turbulent core, yield

$$\frac{\bar{R}_M}{R_V} \ln \frac{p - p_{V_\infty}}{p - p_{V_\delta}} = \frac{\bar{c}_{p_M}}{\bar{c}_{p_V}} \ln \frac{\Delta H + \bar{c}_{p_V} (T_\infty - T_o)}{\Delta H + \bar{c}_{p_V} (T_\delta - T_o)} = \ln \frac{\tau_o + \dot{m}_o u_\infty}{\tau_o + \dot{m}_o u_\delta} \tag{15}$$

Substituting from Equations (6), (7), and (8) in Equation (15),

$$\frac{\bar{c}_{p_M}}{\bar{c}_{p_V}} \ln\left(1 + \frac{\bar{c}_{p_V}(T_\infty - T_o)}{\Delta H}\right) = \ln\left(1 + \frac{\dot{m}_o u_\infty}{\tau_o}\right) + (\bar{Pr}_M - 1)\frac{\dot{m}_o \delta'}{\mu_{M_o}} \qquad (16)$$

$$\frac{\bar{R}_M}{R_V} \ln\left(1 + \frac{p_{V_o} - p_{V_\infty}}{p - p_{V_o}}\right) = \ln\left(1 + \frac{\dot{m}_o u_\infty}{\tau_o}\right) + (\bar{Sc}_M - 1)\frac{\dot{m}_o \delta'}{\mu_{M_o}} \qquad (17)$$

(Note that when $\bar{Pr}_M = \bar{Sc}_M = 1$, Equations (16) and (17) are identical with the results which one obtains when the Reynolds analogy is applied to the entire gas stream including the laminar sublayer. This state of affairs is in accord with the premises upon which the Reynolds analogy was extended.) Equations (16) and (17) provide the desired relations between evaporation rate, fluid properties, and gas-stream parameters.

However, before Equations (16) and (17) can be used conveniently for the calculation of the evaporation rate for given fluid properties and gas-stream parameters, the shear stress at the liquid-gas interface τ_o, the gas-stream laminar sublayer thickness δ', and the vapor pressure at the liquid-gas interface p_{V_o} must be related to easily manipulated parameters. Consider the shear stress τ_o. Not enough experimental data concerning turbulent pipe flows with mass addition at the wall are available to permit one to make a precise prediction of the value of τ_o for given gas-stream and mass-addition parameters. Hence, assume (with Rannie; cf. Reference 12) that the shear stress τ_δ at the junction of the laminar sublayer with the turbulent core is unaffected by mass addition at the wall and is

the same as for ordinary turbulent pipe flows, i.e., that τ_δ can be related to the gas-stream parameters and the ordinary pipe flow friction coefficient C_f by

$$\tau_\delta = \frac{C_f}{2} \rho_\infty u_\infty^2 \tag{18}$$

The consequence of this assumption is that τ_o is now related to gas-stream and mass-addition parameters by

$$\tau_o = \frac{\tau_o}{\tau_\delta} \tau_\delta = e^{-\frac{\dot{m}_o \delta'}{\mu_{M_o}}} \frac{C_f}{2} \rho_\infty u_\infty^2 \tag{19}$$

a relation which includes a simple correction for mass-addition effects and which reduces to the ordinary pipe-flow relation when the mass-addition rate vanishes. It is suggested that C_f be taken to be the friction coefficient corresponding to ordinary turbulent flows in smooth pipes when performing calculations for stable films. (Abramson's remark in Reference 13 implying that friction coefficients for stable liquid wall films are greater than those for smooth pipes is not well founded; the investigations referred to by Abramson, namely, those examined by Lockhart and Martinelli in Reference 20 and Bergelin in Reference 21, were conducted with liquid flows considerably out of the range found in stable liquid wall films.) This treatment of the shearing stress τ_o will most certainly have to be modified (especially for large evaporation rates) when more complete information is available concerning the effects of mass addition on turbulent flows. In the meantime, Equation (19) indicates the trend of the effects of mass addition on shearing stress at the wall.

In analogy with ordinary turbulent pipe flows, identify δ' with the dimensionless laminar sublayer thickness δ^* by means of the defining relation

$$\delta^* = \frac{\rho_\infty \sqrt{\tau_\delta / \rho_\infty}\, \delta'}{\mu_{M_0}} \tag{20}$$

so that the factor $\dot{m}_0 \delta' / \mu_{M_0}$ which appears in Equations (16) and (17) may be written in the form

$$\frac{\dot{m}_0 \delta'}{\mu_{M_0}} = \frac{\dot{m}_0}{\rho_\infty u_\infty} \sqrt{\frac{2}{c_f}}\, \delta^* \tag{21}$$

Here δ^* is a parameter which cannot be evaluated except by experiment. But the laminar sublayer thickness for flow when mass is added at the wall has not been experimentally determined. Hence, a simple extension from results of ordinary pipe-flow experiments will be made. Prandtl (Cf. Reference 22) found that, for ordinary turbulent pipe flows, the assumption

$$\frac{u_\delta}{u_\infty} = \sqrt{\frac{c_f}{2}}\, \frac{\rho \sqrt{\tau_0 / \rho}\, \delta}{\mu} = 1.1 \times Re^{-1/8} \tag{22}$$

fits the experimental results; this assumption has led to the use of

$$\frac{\rho \sqrt{\tau_0 / \rho}\, \delta}{\mu} = 5.6 \tag{23}$$

for ordinary turbulent pipe flows. The simplest assumption for flows with mass addition at the walls which reduces to Equation (23) in the case of flow with no mass addition is

$$\frac{\rho_\infty \sqrt{\tau_\delta / \rho_\infty}\, \delta'}{\mu_{M_0}} = \delta^* = 5.6 \tag{24}$$

In the absence of better information, it is suggested that this relation be used. Note that the treatment of variable viscosity in the gas-stream laminar sublayer provides for laminar-sublayer-thickness corrections due to the effects of variable fluid properties in the direction suggested by Reichardt (Cf. Reference 23).

From the kinetic theory of gases (Cf. Reference 24) the relation connecting the vapor pressure p_{v_o}, the surface temperature T_o, and the evaporation rate $\dot{m}_o$ from the surface is

$$\dot{m}_o = \frac{(p_{v_s} - p_{v_o})\, f}{\sqrt{2\pi R_v T_o}} \tag{25}$$

where f is the evaporation coefficient (equal to or less than unity), and the subscript s refers to saturation conditions corresponding to the surface temperature T_o. In order to indicate the relative magnitudes of p_{v_s} and p_{v_o}, Equation (25) may be rearranged into the form

$$\frac{p_{v_s}}{p_{v_o}} = 1 + \left(\frac{v}{a}\right)_{v_o} \frac{\sqrt{2\pi \gamma_{v_o}}}{f} \tag{25a}$$

where v_v is the diffusion velocity in the y direction of the vapor relative to the evaporating surface, and a_v is the velocity of sound in vapor. Parameter values typical of those encountered in a film-cooling application are f = 0.04 (Cf. Reference 22), $\gamma_{v_o} = 1.3$, and $(v/a)_{v_o} = (1/1750)$. For these parameter values, Equation (25a) reads

$$\frac{p_{v_s}}{p_{v_o}} = 1 + \frac{1}{1750} \frac{\sqrt{2\pi \times 1.3}}{0.04} = 1.04 \tag{25b}$$

so that one may write to good approximation

$$p_{v_o} = p_{v_s} \tag{26}$$

where p_{v_s} is a known function of T_o (Cf., e.g., Reference 25 for tables of experimental data or use Clausius-Clapeyron equation). The relating of the unwieldy parameters r_o, δ', and p_{v_o} to easily manipulated parameters is now completed, and Equations (16) and (17) may be written in the convenient form

$$\frac{\bar{c}_{p_M}}{\bar{c}_{p_V}} \ln\left(1 + \frac{\bar{c}_{p_V}(T_\infty - T_o)}{\Delta H}\right) = \ln\left(1 + \frac{\dot{m}_o}{\rho_\infty u_\infty}\frac{2}{c_f}\right) e^{\frac{\dot{m}_o}{\rho_\infty u_\infty}\sqrt{\frac{2}{c_f}}\,\delta^*}\Bigg) + (\bar{P}_{r_M} - 1)\frac{\dot{m}_o}{\rho_\infty u_\infty}\sqrt{\frac{2}{c_f}}\,\delta^* \quad (27)$$

$$\frac{\bar{R}_M}{R_V} \ln\left(1 + \frac{p_{v_s} - p_{v_\infty}}{p - p_{v_s}}\right) = \ln\left(1 + \frac{\dot{m}_o}{\rho_\infty u_\infty}\frac{2}{c_f}\right) e^{\frac{\dot{m}_o}{\rho_\infty u_\infty}\sqrt{\frac{2}{c_f}}\,\delta^*}\Bigg) + (\bar{S}_{c_M} - 1)\frac{\dot{m}_o}{\rho_\infty u_\infty}\sqrt{\frac{2}{c_f}}\,\delta^* \quad (28)$$

They provide the desired relationship (implicit, to be sure) between evaporation rate (or, alternatively, liquid-film surface temperature), fluid properties, and gas-stream parameters.

Discussion of Solution. Since Equations (27) and (28) reduce to

$$\frac{1}{c_h} = \frac{2}{c_f} + \delta^*\sqrt{\frac{2}{c_f}}\,(P_{r_G} - 1) \quad (29)$$

$$\frac{1}{c_m} = \frac{2}{c_f} + \delta^*\sqrt{\frac{2}{c_f}}\,(S_{c_G} - 1) \quad (30)$$

as $\dot{m}_o$ and p_V approach zero, where the gas-stream, heat-transfer coefficient c_h and the gas-stream, mass-transfer coefficient c_m are in this case defined by

$$c_h = \frac{\dot{q}_o}{\rho_\infty u_\infty \bar{c}_{p_G}(T_\infty - T_o)} = \frac{\dot{m}_o \Delta H}{\rho_\infty u_\infty \bar{c}_{p_G}(T_\infty - T_o)} \quad (31)$$

$$C_m = \frac{\dot{m}_s}{u_\infty (\rho_{v_s} - \rho_{v_\infty}) / R_v T_\infty} \tag{32}$$

it is proposed that Equations (27) and (28) are extensions of the Prandtl-Taylor equation to heat transfer and mass transfer in the case of film cooling.

Note also that, for relatively small temperature and vapor-pressure differences, one may eliminate the evaporation rate from Equations (27) and (28) to obtain

$$\frac{\rho_{v_s}}{\rho - \rho_{v_s}} - \frac{\rho_{v_\infty}}{\rho - \rho_{v_s}} \approx \frac{R_v}{\bar{R}_M} \cdot \frac{\bar{c}_{p_M}(T_\infty - T_o)}{\Delta H} \left[\frac{1 + \sqrt{\frac{c_f}{2}}\, \delta^* (\bar{Sc}_M - 1)}{1 + \sqrt{\frac{c_f}{2}}\, \delta^* (\bar{Pr}_M - 1)} \right] \tag{33}$$

Compare this approximate equation with the semi-empirical, wet-bulb-thermometer equation (valid for small temperature differences and small vapor pressures)

$$\frac{\rho_{v_s}}{\rho - \rho_{v_s}} - \frac{\rho_{v_\infty}}{\rho - \rho_{v_\infty}} = \frac{R_v}{R_G} \cdot \frac{\bar{c}_{p_M}(T_\infty - T_o)}{\Delta H} \left(\frac{\bar{Sc}_M}{\bar{Pr}_M} \right)^{0.56} \tag{34}$$

where

$$\frac{\rho_{v_s}}{\rho - \rho_{v_s}} - \frac{\rho_{v_\infty}}{\rho - \rho_{v_\infty}} = \frac{R_v}{R_G} \cdot \frac{\bar{c}_{p_M}(T_\infty - T_o)}{\Delta H} \tag{35}$$

is the wet-bulb-thermometer equation presented by Lewis (Cf. Reference 26), and

$$\left(\frac{\bar{Sc}_M}{\bar{Pr}_M} \right)^{0.56} \tag{36}$$

is a modifying function based upon the correlation presented by Bedingfield and Drew (Cf. Reference 27) for data which were obtained with Schmidt numbers from 0.60 to 2.60 and Prandtl number equal to 0.70. (Although Klinkenberg and Mooy have given the name Lewis number to the ratio Sc/Pr in Reference 28, this nomenclature is not generally used in current literature.) If the derivation leading up to Equation (33) is correct, then the theoretical factor

$$\left[\frac{1 + \sqrt{\frac{C_f}{2}}\ \delta^* \left(\bar{Sc}_M - 1\right)}{1 + \sqrt{\frac{C_f}{2}}\ \delta^* \left(\bar{Pr}_M - 1\right)} \right] \tag{37}$$

should be approximately equal to the empirical factor

$$\left(\frac{\bar{Sc}_M}{\bar{Pr}_M} \right)^{0.56} \tag{36}$$

for the parameter values upon which the exponent 0.56 was based. A precise comparison of factors (36) and (37) cannot be made since C_f is not precisely known for the test conditions corresponding to the data examined by Bedingfield and Drew. However, one can make a reasonable approximate comparison by noting that, for adiabatic pipe flows at relatively low Reynolds numbers with no mass addition at the wall,

$$\sqrt{\frac{C_f}{2}}\ \delta^* = \frac{u_\delta}{u_\infty} = \sqrt{\frac{0.0791}{2}}\ Re_G^{-1/8}{}^{5.6} \approx \frac{1}{2} \tag{38}$$

and then by accepting this approximation as being also a reasonable approximation for general flows when low mass-transfer rates and small temperature gradients exist (as was the case in the tests

corresponding to the data examined by Bedingfield and Drew). Subsequent calculations based on this approximation (Cf. Figure 14) indicate that the value of factor (36) differs by only an insignificant amount from the value of factor (37) for Schmidt numbers from 0.60 to 2.60 and Prandtl number equal to 0.70. Hence, it is proposed that Equations (27) and (28), taken collectively, constitute an extension of the wet-bulb-thermometer equation to the case when relatively large temperature and partial-pressure gradients occur.

Confusion exists in current literature concerning the value of the surface temperature of a liquid film flowing under the influence of a heated gas stream. (It is especially important to know the value of this temperature when calculating values of the fluid properties at the gas-liquid interface.) Several authors have assumed the liquid-film surface temperature to be equal to the boiling temperature of the liquid under the prevailing static pressure in the duct; this assumption is perhaps an erroneous generalization of the observation that the surface temperature of a film evaporating into an atmosphere consisting of only its own vapor is very nearly equal to the boiling temperature of the liquid under the prevailing pressure. Such a generalization is not valid when the atmosphere into which the liquid film is evaporating contains gases other than the vapor corresponding to the liquid in the film (as is usually the case for film cooling); actually, the following statements hold:

1. The liquid-film surface temperature is very nearly equal to the boiling temperature of the liquid when under a pressure equal to the prevailing interfacial

vapor pressure (Cf. Equation (25a)).

2. The prevailing interfacial vapor pressure is less than the static pressure in the duct (and consequently the liquid-film surface temperature is lower than the boiling temperature of the liquid when under a pressure equal to the static pressure prevailing in the duct), provided that the ratio $\dot{m}_o u_\infty / \tau_o$ is not infinite and that p_{v_∞} is not equal to p (Cf. Equation (17); do not forget assumption 8).

To indicate the effects of several parameter variations on the evaporation rate $\dot{m}_o$ and the liquid-film surface temperature T_o, the curves which are presented in Figures 15 and 16 have been prepared. The figures indicate that, when efficient coolant usage is required for given gas-stream parameters, it is desirable that the coolant have a high specific heat and a large heat of vaporization.

Since it is not possible, in general, to obtain explicit relations for either the evaporation rate $\dot{m}_o$ or the film surface temperature T_o from Equations (27) and (28), curves such as are presented in Figures 15 and 16 are found to be useful aids in the determination of $\dot{m}_o$ and/or T_o for given fluid properties and gas-stream parameters. The following procedure is suggested for obtaining the solution to a general evaporation problem:

1. For the given fluid properties and friction coefficient, prepare a curve of $\dot{m}_o / \rho_\infty u_\infty$ vs $\bar{c}_{p_v} (T_\infty - T_o)/\Delta H$ and a curve of $\dot{m}_o / \rho_\infty u_\infty$ vs $(p_{v_s} - p_{v_\infty})/(p - p_{v_s})$, calculating $\bar{c}_{p_v} (T_\infty - T_o)/\Delta H$ and $(p_{v_s} - p_{v_\infty})/(p - p_{v_s})$ for selected values of $\dot{m}_o / \rho_\infty u_\infty$.

2. Estimate the value of T_o and calculate $\bar{c}_{p_v}(T_\infty - T_o)/\Delta H$ based on this estimation. [Note, for relatively large values of T_∞, that $\bar{c}_{p_v}(T_\infty - T_o)/\Delta H$ varies much more slowly with variations in T_o than does $(p_{v_s} - p_{v_\infty})/(p - p_{v_s})$.]
3. Read $\dot{m}_o/\rho_\infty u_\infty$ from the appropriate prepared curve, using the value of $\bar{c}_{p_v}(T_\infty - T_o)/\Delta H$ calculated in step 2.
4. Read $(p_{v_s} - p_{v_\infty})/(p - p_{v_s})$ from the appropriate prepared curve, using the value of $\dot{m}_o/\rho_\infty u_\infty$ obtained in step 3.
5. Calculate T_o corresponding to the value of $(p_{v_s} - p_{v_\infty})/(p - p_{v_s})$ obtained in step 4.
6. If the value of $\bar{c}_{p_v}(T_\infty - T_o)/\Delta H$ based upon the value of T_o as calculated in step 5 is appreciably different from the value of $\bar{c}_{p_v}(T_\infty - T_o)/\Delta H$ based upon the value of T_o as estimated in step 2, then repeat steps 3, 4, and 5 using the corrected value of $\bar{c}_{p_v}(T_\infty - T_o)/\Delta H$. Such iteration is usually unnecessary when T_∞ is relatively large; then $\bar{c}_{p_v}(T_\infty - T_o)/\Delta H$ is a very slowly varying function of T_o, and $(p_{v_s} - p_{v_\infty})/(p - p_{v_s})$ is a very rapidly varying function of T_o.

Note that calculations are greatly simplified in the event that the Prandtl and Schmidt numbers are nearly equal. In this case the following procedure is suggested for obtaining the solution to a given evaporation problem:

1. Eliminate the evaporation rate from Equations (27) and (28) to obtain a relatively simple relation between T_∞ and functions of T_o (which relation is independent of flow parameters)

$$\frac{\bar{c}_{p_M}}{\bar{c}_{p_V}} \ln\left(1 + \frac{\bar{c}_{p_V}(T_\infty - T_o)}{\Delta H}\right) = \frac{\bar{R}_M}{R_V} \ln\left(1 + \frac{p_{V_s} - p_{V_\infty}}{p - p_{V_s}}\right) \qquad (39)$$

Prepare curves of T_o vs T_∞ and a curve of $\dot{m}_o/\rho_\infty u_\infty$ vs $\bar{c}_{p_V}(T_\infty - T_o)/\Delta H$ for the given conditions, calculating T_∞ for selected values of T_o and $\bar{c}_{p_V}(T_\infty - T_o)/\Delta H$ for selected values of $\dot{m}_o/\rho_\infty u_\infty$.

2. Read T_o from the appropriate prepared curve, using the given value of T_∞.
3. Calculate $\bar{c}_{p_V}(T_\infty - T_o)/\Delta H$, using the value of T_o obtained in step 2.
4. Read $\dot{m}_o/\rho_\infty u_\infty$ from the appropriate prepared curve, using the value of $\bar{c}_{p_V}(T_\infty - T_o)/\Delta H$ calculated in step 3.

Evaporation rates predicted by Equation (27) of this paper

$$\frac{\bar{c}_{p_M}}{\bar{c}_{p_V}} \ln\left(1 + \frac{\bar{c}_{p_V}(T_\infty - T_o)}{\Delta H}\right) = \ln\left(1 + \frac{\dot{m}_o}{\rho_\infty u_\infty} \frac{2}{c_f} e^{\frac{\dot{m}_o}{\rho_\infty u_\infty}\sqrt{\frac{2}{c_f}}\delta^*}\right) + \left(\bar{\rho}_{r_M} - 1\right)\frac{\dot{m}_o}{\rho_\infty u_\infty}\sqrt{\frac{2}{c_f}}\delta^* \qquad (27)$$

are compared in Figure 17 with those predicted by Crocco's extension of Rannie's equation to the case of film cooling, which equation (in the present nomenclature) reads

$$\frac{\bar{c}_{p_M}}{\bar{c}_{p_V}} \ln\left(1 + \frac{\bar{c}_{p_V}(T_\infty - T_0)}{\Delta H}\right) = \frac{\bar{c}_{p_M}}{\bar{c}_{p_V}} \ln\left[e^{\frac{\dot{m}_0}{\rho_\infty u_\infty}\sqrt{\frac{2}{c_f}}\,\delta^*} + \frac{\bar{c}_{p_V}}{\bar{c}_{p_M}}\left(\frac{1}{\delta^*}\sqrt{\frac{2}{c_f}}\right.\right.$$

$$\left.\left. - 1\right)\left(e^{\frac{\dot{m}_0}{\rho_\infty u_\infty}\sqrt{\frac{2}{c_f}}\,\delta^*} - 1\right)\right] + \left(\bar{P}r_M - \frac{\bar{c}_{p_M}}{\bar{c}_{p_V}}\right)\frac{\dot{m}_0}{\rho_\infty u_\infty}\sqrt{\frac{2}{c_f}}\,\delta^* \qquad (40)$$

The divergence of the two curves is due to the fact that effects of mass addition on transport phenomena in the turbulent core have been treated differently in the two analyses.

Summarizing, a method has been found for determining the evaporation rate and the surface temperature for a stable inert liquid wall film flowing under the influence of a high-velocity, fully developed turbulent gas stream in a duct. The method is based upon extensions of the Prandtl-Taylor equation to heat transfer and mass transfer in the case of film cooling which collectively constitute an extension of the wet-bulb-thermometer equation to the case when large temperature and partial-pressure gradients occur. An attempt has been made to take into account the effects of mass addition on transport phenomena in the turbulent core.

V-B: Experimental Study

The data which were presented in Figures 6 and 7 (Cf. also Table I) and discussed in Part IV with respect to film stability are discussed in this part with respect to evaporation rate. The evaporation rates which are examined are those which correspond to the longest stable films obtainable for the several sets of gas-stream conditions. It is useless to examine the evaporation rates from unstable films since the mass-transfer rate from unstable films has not been analyzed theoretically; shorter films will not be examined since they are more susceptible to large experimental errors than are long films.

Theoretical values of $\dot{m}_o / \rho_\infty u_\infty$ (Cf. Table IV) were obtained with the aid of Figures 11 and 18, prepared in accordance with Equations (39) and (27), respectively. To obtain $\dot{m}_o / \rho_\infty u_\infty$ for given gas-stream conditions, read the film surface temperature T_o from Figure 11 for the given gas-stream static pressure and bulk temperature, then calculate the heat-transfer parameter $\bar{c}_{p_v} (T_\infty - T_o)/\Delta H$ (a function of T_∞ and T_o), and finally read the mass-flow ratio from Figure 18 for the appropriate value of $\bar{c}_{p_v} (T_\infty - T_o)/\Delta H$ and the given value of C_f . (Figure 11, incidentally, emphasizes that, in general, although T_∞ may be much greater than the boiling temperature of the liquid at the prevailing pressure, the boiling point of the liquid is not necessarily reached at the liquid surface; cf. Part V-A.)

A preliminary examination of the available data (that reported in this paper and that summarized by Kinney in Reference 11) discloses that the realized evaporation rates consistently exceeded

the predicted values (Cf. Table IV). The reason for this discrepancy becomes apparent when assumption 8 of Part V-A is compared with the test conditions which existed. Whereas it was assumed that axial variations in the gas stream were small compared with radial variations, test conditions were such that extremely large axial variations occurred at the point of liquid injection, i.e., at the test-section inlet; although the velocity profile at the test-section inlet was essentially that of fully developed turbulent pipe flow (since approach duct lengths of 10 and 20 pipe diameters were employed by Kinney, and approach duct lengths of 27 pipe diameters were employed in the current tests), the partial-pressure and temperature profiles at the test-section inlet were essentially square (since the air was virtually dry upstream from the test-section inlet and the approach duct was thermally insulated). Consequently, one would be surprised if the experimentally determined evaporation rates did not exceed the predicted values.

Calculations by Latzko (Cf. Reference 29) and experimental data by Boelter, Young, and Iverson (Cf. Reference 30) indicate that, when the temperature profile at the test-section inlet is that for fully developed turbulent pipe flow, then the ratio of the average heat-transfer coefficient for a finite-length heated test section (whose length is at least five times its diameter) to the local heat-transfer coefficient far downstream from the inlet of an infinitely long heated test section may be given by an expression of the form

$$1 + \text{CONSTANT} \times Re_G^{0.25} (d/L)$$

where d is the duct diameter and L is the test-section length. (For

air flows in polished tubes with no mass diffusion, Boelter et al determined the value of the constant to be approximately 0.1.) These results motivated Figure 19, where experimentally determined values of $\dot{m}_o / \rho_\infty u_\infty$ are plotted as a function of calculated values of $\dot{m}_o / \rho_\infty u_\infty$ which have been multiplied by the parameter $1 + (1/3)Re_G^{0.25}(d/L)$. (Gas properties have been evaluated at the bulk temperature T_∞; in the event that the bulk temperature is extremely large compared with the wall temperature, it may be necessary to evaluate the gas properties at the average of the bulk and wall temperatures instead of at the bulk temperature, as suggested by Deissler in Reference 31.) Figure 19 explains the excessively large evaporation rates found to occur for the very short films (Cf. Figures 6 and 7 of this paper and Figure 4 of Reference 11) and implies that even greater modifications of evaporation rates as predicted by Equations (27) and (28) will be necessary if the velocity profile at the test-section inlet is square as are also the partial-pressure and temperature profiles (Cf. Reference 30 for experimental data on the effects of various entrance conditions on heat-transfer coefficients for turbulent flows of gases in ducts).

The relative merits of Equation (27) and Crocco's equation cannot be compared with existing experimental data since (a) the parameter $\bar{c}_{p_V}(T_\infty - T_o)/\Delta H$ did not exceed unity in either the NACA or the present tests and (b) the evaporation rates predicted by Equation (27) and Crocco's equation do not deviate appreciably until the parameter $\bar{c}_{p_V}(T_\infty - T_o)/\Delta H$ exceeds unity (Cf. Figure 17).

Since the combined thickness of the duct wall and the liquid

film was relatively small (less than 0.1 inch) and the heat-transfer rate from the test section to its environment was small, the duct wall temperature was taken to be approximately equal to the film-surface temperature. Hence, the measured wall temperatures have been plotted in Figure 11 for comparison with predicted film-surface temperatures at 1 atmosphere (test pressures ranged from 14.2 to 16.7 psia; cf. Table V). The data agree with the theoretical curve with a maximum error of $6^{\circ}R$. Inasmuch as the data were taken at relatively large partial-pressure and temperature gradients (the parameter $(p_{V_s} - p_{V_\infty})/(p - p_{V_s})$ exceeded 0.7, and the parameter $\overline{c_{p_V}}(T_\infty - T_o)/\Delta H$ exceeded 0.9 in some of the tests), it is concluded that the data support the proposal of Section V-A that Equations (27) and (28), taken collectively, constitute an extension of the wet-bulb-thermometer equation to the case when relatively large temperature and partial-pressure gradients occur.

Summarizing, experimental data concerning evaporation rates from stable liquid wall films into heated turbulent gas streams were brought into agreement with calculated evaporation rates after corrections for entrance effects were made. Good agreement was realized between predicted and measured liquid wall film temperatures.

The present investigation has re-emphasized the fact that information concerning the effects of entrance conditions on the transfer of heat, mass, and momentum in pipe flows is scarce. It would be useful to extend previous studies (Cf. References 29 and 30) of the effects of various entrance conditions on transport phenomena in pipe flows analytically and experimentally.

Reynolds-analogy extensions of the type proposed in Part V-A are potentially useful in the analyses of several important processes (e.g., combustion, evaporation, and jet mixing) which involve transport phenomena in turbulent gas streams. However, the proposed treatment of mass-addition effects on transport phenomena in the turbulent core of pipe flows has not been confirmed; i.e., the relative merits of Equation (27) and Crocco's equation have not been established. Consequently, further studies are required to determine the correctness of hypotheses of the type expressed by Equation (27).

REFERENCES

1. Goddard, Robert H., Rocket Development. New York: Prentice-Hall, Inc., 1948.

2. Zucrow, M. J., "Liquid Propellant Rocket Power Plants," Transactions ASME, 69:847-857, November, 1947.

3. Zucrow, M. J., Beighley, C. M., and Knuth, E., Progress Report on the Stability of Liquid Films for Cooling Rocket Motors, Technical Report No. 23. Lafayette (Ind.): Purdue University, November, 1950.

4. Project Squid, Semi-Annual Progress Report, April 1, 1952.

5. Greenberg, Arthur B., The Stability and Flow of Liquid Films Injected into an Air Duct Through Spaced Parallel Disks in the Two- and Three-Dimensional Cases (Master of Science Thesis in Aeronautical Engineering). Lafayette (Ind.): Purdue University, August, 1952.

6. Kinney, George R., and Abramson, Andrew E., Investigation of Annular Liquid Flow with Concurrent Air Flow in Horizontal Tubes, Research Memorandum No. E51C13. Cleveland: National Advisory Committee for Aeronautics, May, 1951.

7. Kinney, George R., and Sloop, John L., Internal Film Cooling Experiments in 4-Inch Duct with Gas Temperatures to 2000°F, Research Memorandum No. E50F19. Cleveland: National Advisory Committee for Aeronautics, September, 1950.

8. Deissler, Robert G., Analytical and Experimental Investigation of Adiabatic Turbulent Flow in Smooth Tubes, Technical Note No. 2138. Cleveland: National Advisory Committee for Aeronautics, July, 1950.

9. Colburn, A. P., and Carpenter, F. G., The Effect of Vapor Velocity in Condensation Inside Tubes, NEPA Heat Transfer Lectures, vol 2. Washington: Superintendent of Documents, June 1, 1949.

10. Crocco, L., "An Approximate Theory of Porous, Sweat, or Film Cooling with Reactive Fluids," Journal of the American Rocket Society, 22 (No. 6):331-338, November-December, 1952.

11. Kinney, George R., Internal-Film-Cooling Experiments with 2- and 4-Inch Smooth-Surface Tubes and Gas Temperatures to 2000°F, Research Memorandum No. E52B20. Cleveland: National Advisory Committee for Aeronautics, April, 1952.

12. Rannie, W. D., A Simplified Theory of Porous Wall Cooling, Progress Report No. 4-50. Pasadena: Jet Propulsion Laboratory, California Institute of Technology, November 24, 1947.

13. Abramson, Andrew E., "Comment on 'An Approximate Theory of Porous, Sweat, or Film Cooling with Reactive Fluids' by L. Crocco," Journal of the American Rocket Society, 23 (No. 2): 97, March-April, 1953.

14. Knuth, Eldon L., A Study of the Mechanics of Liquid Films As Applied to Film Cooling, Progress Report No. 1-79. Pasadena: Jet Propulsion Laboratory, California Institute of Technology, November 21, 1951.

15. Shapiro, Ascher H., and Hawthorne, W. R., "The Mechanics and Thermodynamics of Steady One-Dimensional Gas Flow," Journal of Applied Mechanics, December, 1947, pp. A-317 to A-336.

16. Bromley, L. A., and Wilke, C. R., "Viscosity Behavior of Gases," Industrial and Engineering Chemistry, 43 (No. 7): 1641-1648, July, 1951.

17. Tietjens, O., "Beiträge zur Entstehung der Turbulenz," ZAMM, Band 5 (Heft 3): 200-217, Juni, 1925.

18. Wuest, W., "Beitrag zur Entstehung von Wasserwellen durch Wind," ZAMM, Band 29 (Heft 7/8):239:252, Juli/August, 1949.

19. Reynolds, Osborne, "On the Extent and Action of the Heating Surface of Steam Boilers," Proceedings of the Literary and Philosophical Society of Manchester, vol 14, 1874. Reprinted in Scientific Papers of Osborne Reynolds, 1:81-85. New York: Cambridge University Press, 1900.

20. Lockhart, R. W., and Martinelli, R. C., "Proposed Correlation of Data for Isothermal Two-Phase, Two-Component Flow in Pipes," Chemical Engineering Progress, 45:39-48, January, 1949.

21. Bergelin, O. P., "Flow of Gas-Liquid Mixtures," Chemical Engineering, 56:104-106, May, 1949.

22. Prandtl, L., "Bemerkung über die Wärmeübergang im Rohr," Physikalische Zeitschrift, 29:487-489, 1928.

23. Reichardt, H., "Die Wärmeübertragung in turbulenten Reibungsschichten," ZAMM, Band 20(Heft 6):297-328, December, 1940.

24. Alty, T., "The Maximum Rate of Evaporation of Water," Philosophical Magazine and Journal of Science, 15:82-103, 1933.

25. International Critical Tables. New York: McGraw-Hill Book Company, 1926.

26. Lewis, W. K., "The Evaporation of a Liquid into a Gas," Transactions ASME, 44:325-340, 1922.

27. Bedingfield, Charles H., Jr., and Drew, Thomas B., "Analogy Between Heat Transfer and Mass Transfer -- a Psychrometric Study," Ind. and Eng. Chem., 42:1164-1173, June, 1950.

28. Klinkenberg, A., and Mooy, H. H., "Dimensionless Groups in Fluid Friction, Heat, and Material Transfer," Chemical Engineering Progress, 44:17-36, January, 1948.

29. Latzko, H., "Der Wärmeübergang an einem turbulenten Flüssigkeits oder Gasstrom," ZAMM, Band 1 (Heft 4):268-290, 1921.

30. Boelter, L. M. K., Young, G., and Iverson, H. W., An Investigation of Aircraft Heaters. XXVII - Distribution of Heat-Transfer Rate in the Entrance Section of a Circular Tube, Technical Note No. 1451. Berkeley: National Advisory Committee for Aeronautics, July, 1948.

31. Deissler, Robert G., Analytical Investigation of Turbulent Flow in Smooth Tubes with Heat Transfer with Variable Fluid Properties for Prandtl Number of 1, Technical Note No. 2242. Cleveland: National Advisory Committee for Aeronautics, December, 1950.

32. Reynolds, Osborne, "On the Dynamical Theory of Incompressible Viscous Fluids and the Determination of the Criterion," Phil. Trans., A186:123-164, 1895.

33. Chapman, S., and Cowling, T. G., The Mathematical Theory of Non-Uniform Gases. London: Cambridge University Press, 1952.

APPENDIX A

It has been noted that, for the case of evaporation from an annular liquid wall film into a heated gas stream flowing in a duct, curves of the test-section pressure drop vs liquid-flow rate (or vs protected-surface area) possess abrupt changes in slope which are related to film-attachment efficiency and film stability. This phenomenon is explained by the equations of steady one-dimensional gas flow as developed by Shapiro and Hawthorne (Cf. Reference 15). (Although pipe flows are not identical with one-dimensional flows, the two flows are similar to the extent that many of the properties of pipe flows are qualitatively described by results of an analysis of one-dimensional flows.) With the assumptions that no heat is exchanged with the surroundings by conduction, no area change occurs, flow is one-dimensional, the gas obeys the perfect-gas law, and no molecular-weight change occurs, one may write (with Shapiro and Hawthorne) the variation of pressure in the axial direction in the form

$$\frac{dp}{dx} = -\frac{\gamma_M Ma_M^2}{1-Ma_M^2}\frac{4p}{d}\frac{c_f}{2}\left[1+(\gamma_M-1)Ma_M^2\right]$$

$$+\frac{\gamma_M Ma_M^2}{1-Ma_M^2}\frac{4p}{d}\frac{\dot{m}_a}{\rho_M u}\left[\frac{\Delta H + \bar{c}_{p_v}(T_\infty - T_o) - 2c_{p_M}T_\infty - u^2/2g}{c_{p_M}T_\infty}\right] \qquad \text{(A-1)}$$

where Ma is Mach number, γ is specific heat ratio, and g is acceleration of gravity. The presence of the second term on the right side of the equation indicates that, when vapor is added to the gas

stream and $\Delta H + \bar{c}_{p_V}(T_\infty - T_o) > 2 c_{p_M} T_\infty - u^2/2g$ (as was always the case for the tests described in this paper), the pressure drop for the test section is less than when no vapor is added to the gas stream; i. e., the effect of the addition of mass is to decrease the momentum of the gas stream as a direct result of the transfer of heat from the gas stream to the added mass. Thus Equation (A-1) implies that the magnitude by which the pressure drop for the test section is decreased by the addition of vapor depends upon the rate at which vapor is added to the gas stream and the extent to which the vapor mixes with the gas stream, i. e., ultimately, on the coolant-flow rate, the efficiency of the film-attachment process, and the gas-liquid interfacial conditions.

APPENDIX B

MATHEMATICAL REPRESENTATION OF TRANSPORT PHENOMENA IN TURBULENT CORE OF TWO-COMPONENT PIPE FLOWS WITH UNIDIRECTIONAL RADIAL DIFFUSION

The mass-transfer rate $\dot{m}$, the heat-transfer rate (due to temperature gradient) $\dot{q}$, and the shearing stress τ will be identified with time averages of turbulent fluctuations for the case of unidirectional diffusion of a vapor into a gas flowing in a pipe. The procedure which will be followed is similar to that which was used by Reynolds when he identified the turbulent shearing stress with time averages of turbulent fluctuations for the case of turbulent one-component flows (Cf. Reference 32).

Neglecting static-pressure variations, the conservation of vapor molecules in axially symmetric flows of gas-vapor mixtures in pipes may be described by the partial-differential equation

$$\frac{\partial \pi_V}{\partial t} + \nabla \cdot (\underline{v}_V \pi_V) = 0 \qquad \text{(B-1)}$$

where t is time, $\underline{v}_\kappa$ is the mean velocity of the molecules of species κ, and π_κ (defined by $\pi_\kappa = \rho_\kappa / \rho$) is the relative concentration of molecules of species κ (Cf. Reference 33, Equation 8.1,4). To facilitate the distinguishing of terms arising as the result of molecular processes from terms arising as the result of turbulent processes, add the identity $\nabla \cdot (\underline{v}_G \pi_V - \underline{v}_G \pi_V) \equiv 0$ to Equation (B-1), thereby obtaining

$$\frac{\partial \pi_V}{\partial t} + \nabla \cdot \left[\pi_V (\underline{v}_V - \underline{v}_G) + \pi_V \underline{v}_G \right] = 0 \qquad \text{(B-2)}$$

or, in more convenient form,

$$\frac{\partial \pi_V}{\partial t} + \nabla \cdot \left[D \nabla \ln (1 - \pi_V) + \pi_V \underline{c}_G \right] = 0 \qquad \text{(B-3)}$$

The fluctuating parameters for fully established turbulent flow are $\pi_V = \bar{\pi}_V + \pi_V'$, $u_G = \bar{u}_G + u'$, and $v_G = v'$, where u_G and v_G are respectively, the axial and radial components of $\underline{c}_G$, the barred quantities are quantities averaged with respect to time (functions of position alone), and the primed quantities are turbulent fluctuations. Substituting in Equation (B-3), averaging with respect to time, and neglecting derivatives with respect to time, one obtains

$$\frac{\partial}{\partial x}\left[D \frac{\partial}{\partial x} \ln (1 - \bar{\pi}_V) + \bar{\pi}_V \bar{u}_G + \overline{\pi_V' u'} \right]$$

$$+ \frac{1}{r_o - y} \frac{\partial}{\partial y}\left\{ (r_o - y)\left[D \frac{\partial}{\partial y} \ln (1 - \bar{\pi}_V) + \overline{\pi_V' v'} \right] \right\} = 0 \qquad \text{(B-4)}$$

where x is distance in the axial direction and r_o is the pipe radius. (Note that terms arising as the result of molecular processes are now easily distinguishable from terms arising as the result of turbulent processes.) For convenience, divide the flow within the duct into two regions, a center core in which the fluid flow is predominantly turbulent and a laminar sublayer (adjacent to the duct wall) in which the fluid flow is predominantly laminar. (Comparisons of heat-transfer rates obtained for turbulent pipe flows with heat-transfer rates predicted by the Prandtl-Taylor equation justify such a division into two regions when the Prandtl and Schmidt numbers do not vary from unity by more than a factor of 2. Most gases satisfy this restriction.) Considering the turbulent core only, one

may neglect the terms

$$\frac{\partial}{\partial x}\left[\mathcal{D}\frac{\partial}{\partial x}\ln(1-\bar{\pi}_V)\right] \quad \text{and} \quad \frac{1}{r_o-y}\frac{\partial}{\partial y}\left\{(r_o-y)\left[\mathcal{D}\frac{\partial}{\partial y}\ln(1-\bar{\pi}_V)\right]\right\}$$

of Equation (B-4) in comparison with other terms since mass transfer by molecular diffusion is overshadowed by turbulent effects. One may also neglect the term $\frac{\partial}{\partial x}(\overline{\pi'_V u'})$ in comparison with other terms if the axial partial-pressure and velocity gradients are small compared with the radial gradients. The remaining derivative in the x direction must be retained, however, in order to allow for the addition of vapor molecules at the wall. Then the equation for conservation of vapor molecules reads

$$\frac{\partial}{\partial x}\left[\bar{\pi}_V \bar{u}_G\right] + \frac{1}{r_o-y}\frac{\partial}{\partial y}\left[(r_o-y)\,\overline{\pi'_V v'}\right] = 0 \qquad \text{(B-5)}$$

Noting that the vapor balance for a cylindrical portion of the turbulent core with length dx and radius (r_o - y) may be described by

$$\dot{m}_V\, 2\pi (r_o-y)\, dx = \frac{p}{R_V T}\int_0^{r_o-y} 2\pi (r_o-y)\frac{\partial}{\partial x}(\bar{\pi}_V \bar{u}_G)\, dx\, d(r_o-y) \qquad \text{(B-6)}$$

one may integrate Equation (B-5) with the result

$$\dot{m}_V = \frac{p}{R_V T}\,\overline{\pi'_V v'} \qquad \text{(B-7)}$$

A similar treatment of the continuity equation for gas molecules leads to the result

$$\dot{m}_G = \frac{p}{R_G T}\,\overline{\pi'_G v'} = 0 \qquad \text{(B-8)}$$

where $\dot{m}_G$ is equated to zero since no gas crosses the duct wall. Equations (B-7) and (B-8) constitute the first of the three identifications which are sought.

Neglecting body forces, one may describe the conservation of energy in axially symmetric flows of gas-vapor mixtures in pipes by the partial-differential equation

$$\frac{\partial}{\partial t} \sum \frac{p}{R_\kappa T} \pi_\kappa H_\kappa + \nabla \cdot \left(\sum \frac{p}{R_\kappa T} \pi_\kappa H_\kappa \underline{c}_\kappa - k \nabla T \right) = \Phi + \frac{D p}{\partial t} \quad \text{(B-9)}$$

where Φ represents terms arising as a result of viscous dissipation (Cf. Reference 33, Equation 8.1, 8). Neglecting viscous dissipation and pressure terms and writing diffusion velocities in terms of partial-pressure gradients as before,

$$\frac{\partial}{\partial t} \sum \frac{p}{R_\kappa T} \pi_\kappa H_\kappa + \nabla \cdot \left(\frac{p D}{R_v T} H_v \nabla \ln (1 - \pi_v) \right.$$

$$\left. + \sum \frac{p}{R_\kappa T} \pi_\kappa H_\kappa \underline{c}_G - k \nabla T \right) = 0 \quad \text{(B-10)}$$

It is assumed that the effect of the fluctuations of the ratio p/T due to turbulence are negligible compared with the effect of concentration fluctuations. Noting that $1 - \pi_v = \pi_G$, substituting $\pi_\kappa = \bar{\pi}_\kappa + \pi_\kappa'$, $H_\kappa = \bar{H}_\kappa + H_\kappa'$, $u_\kappa = \bar{u}_\kappa + u'$, $v_\kappa = v'$, and $T = \bar{T} + T'$ in Equation (B-10), averaging with respect to time, and neglecting derivatives with respect to time,

$$\frac{\partial}{\partial x}\left[\frac{pD}{R_v T}\left(\bar{H}_v \frac{\partial}{\partial x}\ln \bar{\pi}_G + \overline{H'_v \frac{\partial}{\partial x}(\pi'_G/\bar{\pi}_G)}\right) + \sum \frac{p}{R_\kappa T}\left(\bar{\pi}_\kappa \bar{H}_\kappa \bar{u}_G + \bar{\pi}_\kappa \overline{H'_\kappa u'} + \bar{H}_\kappa \overline{\pi'_\kappa u'} + \bar{u}_G \overline{\pi'_\kappa H'_\kappa}\right) - k\frac{\partial}{\partial x}\bar{T}\right]$$

$$+\frac{1}{r_o - y}\frac{\partial}{\partial y}\left\{(r_o - y)\left[\frac{pD}{R_v T}\left(\bar{H}_v \frac{\partial}{\partial y}\ln \bar{\pi}_G + \overline{H'_v \frac{\partial}{\partial y}(\pi'_G/\bar{\pi}_G)}\right)\right.\right.$$

$$\left.\left.+\sum \frac{p}{R_\kappa T}\left(\bar{\pi}_\kappa \overline{H'_\kappa v'} + \bar{H}_\kappa \overline{\pi'_\kappa v'}\right) - k\frac{\partial}{\partial y}\bar{T}\right]\right\} = 0 \qquad \text{(B-11)}$$

In comparison with other terms, one may neglect the terms

$$\frac{\partial}{\partial x}\left[\frac{pD}{R_v T}\left(\bar{H}_v \frac{\partial}{\partial x}\ln \bar{\pi}_G + \overline{H'_v \frac{\partial}{\partial x}(\pi'_G/\bar{\pi}_G)}\right)\right]$$

and

$$\frac{1}{r_o - y}\frac{\partial}{\partial y}\left\{(r_o - y)\left[\frac{pD}{R_v T}\left(\bar{H}_v \frac{\partial}{\partial y}\ln \bar{\pi}_G + \overline{H'_v \frac{\partial}{\partial y}(\pi'_G/\bar{\pi}_G)}\right)\right]\right\}$$

since molecular processes are overshadowed by turbulent effects, and the terms

$$\frac{\partial}{\partial x}\left[\sum \frac{p}{R_\kappa T}\left(\bar{\pi}_\kappa \overline{H'_\kappa u'} + \bar{H}_\kappa \overline{\pi'_\kappa u'} + \bar{u}_G \overline{\pi'_\kappa H'_\kappa}\right) - k\frac{\partial}{\partial x}\bar{T}\right]$$

if the axial partial-pressure, temperature, and velocity gradients are small compared with radial gradients. The remaining derivative in the x direction must be retained, however, in order to allow for the addition of heat at the wall. Now the heat-conservation equation reads

$$\frac{\partial}{\partial x}\left[\sum \frac{p}{R_\kappa T}\,\bar{\pi}_\kappa \bar{H}_\kappa \bar{u}_G\right] + \frac{1}{r_o - y}\,\frac{\partial}{\partial y}\left[(r_o - y)\sum \frac{p}{R_\kappa T}\left(\bar{\pi}_\kappa \overline{H'_\kappa v'}\right.\right.$$

$$\left.\left. + \bar{H}_\kappa \overline{\pi'_\kappa v'}\right)\right] = 0 \qquad \text{(B-12)}$$

Noting that the heat balance for a cylindrical portion of the turbulent core with length dx and radius (r_o - y) may be described by

$$\left(\dot{q} + \dot{m}\bar{H}_v\right) 2\pi (r_o - y)\,dx = \int_0^{r_o - y} 2\pi (r_o - y)\,\frac{\partial}{\partial x}\left(\sum \frac{p}{R_\kappa T}\,\bar{\pi}_\kappa \bar{H}_\kappa \bar{u}_G\right) dx\, d(r_o - y) \qquad \text{(B-13)}$$

one may integrate Equation (B-12) with the result

$$\dot{q} + \dot{m}_v \bar{H}_v = \sum \frac{p}{R_\kappa T}\left(\bar{\pi}_\kappa \overline{H'_\kappa v'} + \bar{H}_\kappa \overline{\pi'_\kappa v'}\right) \qquad \text{(B-14)}$$

But from Equation (B-8), $\overline{\pi'_G v'} = 0$; hence,

$$\dot{q} + \dot{m}_v \bar{H}_v = \bar{\rho}_M \overline{H'_M v'} + \frac{p}{R_v T}\,\overline{\pi'_v v'}\,\bar{H}_v \qquad \text{(B-15)}$$

so that the radial heat-transfer rate (due to temperature gradient) $\dot{q}$ is identified with time averages of turbulent fluctuations, after substituting from Equation (B-7), by the relation

$$\dot{q} = \bar{\rho}_m \overline{H'_M v'} \qquad \text{(B-16)}$$

This equation is the second of the three identifications which are sought.

Conservation of axial momentum in axially symmetric flows of gas-vapor mixtures in pipes may be described by the partial-

differential equation

$$\frac{\partial}{\partial t}\sum \frac{p}{R_K T}\,\pi_K u_K + \nabla\cdot\left(\sum \frac{p}{R_K T}\,\pi_K \zeta_K u\right) = -\nabla p + \nabla\cdot(\mu_M \nabla u) \qquad \text{(B-17)}$$

(Cf. Reference 33, Equation 8.1,7). Writing diffusion velocities in terms of partial-pressure gradients as before,

$$\frac{\partial}{\partial t}\left[\frac{p}{R_V T}\,D\,\frac{\partial}{\partial x}\ln(1-\pi_V) + \sum \frac{p}{R_K T}\,\pi_K u_G\right] + \nabla\cdot\left[\frac{pu}{R_V T}\,D\,\nabla \ln(1-\pi_V)\right.$$

$$\left. + \sum \frac{pu}{R_K T}\,\pi_K \zeta_G\right] = -\nabla p + \nabla\cdot(\mu_M \nabla u) \qquad \text{(B-18)}$$

Neglecting fluctuations of p/T, substituting $\pi_K = \bar{\pi}_K + \pi_K'$, $u_G = \bar{u}_G + u'$, $v_K = v'$, $p = \bar{p} + p'$, and $u = \bar{u} + u'$ in Equation (B-18), averaging with respect to time, and neglecting derivatives with respect to time,

$$\frac{\partial}{\partial x}\left[\frac{pD}{R_V T}\left(\bar{u}\,\frac{\partial}{\partial x}\ln\bar{\pi}_G + \overline{u'\frac{\partial}{\partial x}(\pi_G'/\bar{\pi}_G)}\right) + \sum \frac{p}{R_K T}\left(\bar{u}\,\bar{\pi}_K\bar{u}_G\right.\right.$$

$$\left.\left. + \bar{u}\,\overline{\pi_K' u'} + \bar{\pi}_K\,\overline{u'u'} + \bar{u}_G\,\overline{\pi_K' u'}\right)\right] + \frac{1}{r_o - y}\,\frac{\partial}{\partial y}\left\{(r_o - y)\left[\frac{pD}{R_V T}\left(\bar{u}\,\frac{\partial}{\partial y}\ln\bar{\pi}_G\right.\right.\right.$$

$$\left.\left.\left. + \overline{u'\frac{\partial}{\partial y}(\pi_G'/\bar{\pi}_G)}\right) + \sum \frac{p}{R_K T}\left(\bar{u}\,\overline{\pi_K' v'} + \bar{\pi}_K\,\overline{u'v'}\right)\right]\right\}$$

$$= -\frac{\partial \bar{p}}{\partial x} + \frac{\partial}{\partial x}\left(\mu_M \frac{\partial \bar{u}}{\partial x}\right) + \frac{1}{r_o - y}\,\frac{\partial}{\partial y}\left[(r_o - y)\,\mu_M \frac{\partial \bar{u}}{\partial y}\right]$$

(B-19)

In comparison with other terms, one may neglect the terms

$$\frac{\partial}{\partial x}\left[\frac{pD}{R_v T}\left(\bar{u}\frac{\partial}{\partial x}\ln\bar{\pi}_G + \overline{u'\frac{\partial}{\partial x}\left(\pi'_G/\bar{\pi}_G\right)}\right)\right]$$

and

$$\frac{1}{r_o-y}\frac{\partial}{\partial y}\left\{(r_o-y)\left[\frac{pD}{R_v T}\left(\bar{u}\frac{\partial}{\partial y}\ln\bar{\pi}_G + \overline{u'\frac{\partial}{\partial y}\left(\pi'_G/\bar{\pi}_G\right)}\right)\right]\right\}$$

since molecular processes are overshadowed by turbulent effects, and the terms

$$\frac{\partial}{\partial x}\left[\sum\frac{p}{R_K T}\left(\bar{u}\,\bar{\pi}_K\bar{u}_G + \bar{u}\,\overline{\pi'_K u'} + \bar{\pi}_K\overline{u'u'} + \bar{u}_G\overline{\pi'_K u'}\right) - \mu_M\frac{\partial\bar{u}}{\partial x}\right]$$

if the axial partial-pressure and velocity gradients are small compared with radial gradients. The term $\partial\bar{p}/\partial x$ must be retained, however, in order to allow for effects of shearing stress and mass transfer at the wall. Now the momentum conservation equation reads

$$\frac{\partial}{\partial y}\left[(r_o-y)\sum\frac{p}{R_k T}\left(\bar{u}\,\overline{\pi'_K v'} + \bar{\pi}_K\overline{u'v'}\right)\right] = -(r_o-y)\frac{\partial\bar{p}}{\partial x} \qquad \text{(B-20)}$$

Noting that the force balance for a cylindrical portion of the turbulent core with length dx and radius (r_o - y) may be described by

$$(-\tau + \dot{m}_v\bar{u})\,2\pi(r_o-y)\,dx = \int_o^{r_o-y} 2\pi(r_o-y)\frac{\partial\bar{p}}{\partial x}\,dx\,d(r_o-y) \qquad \text{(B-21)}$$

one may integrate Equation (B-20) with the result

$$-\tau + \dot{m}_v\bar{u} = \sum\frac{p}{R_K T}\left(\bar{\pi}_K\overline{u'v'} + \bar{u}\,\overline{\pi'_K v'}\right) \qquad \text{(B-22)}$$

But from Equation (B-8), $\overline{\pi'_G v'} = 0$; hence,

$$-\tau + \dot{m}_v \bar{u} = \bar{\rho}_M \overline{u'v'} + \frac{p}{R_v T} \overline{\pi'_v v'} \bar{u} \qquad \text{(B-23)}$$

so that the shearing stress τ is identified with time averages of turbulent fluctuations, after substituting from Equation (B-7), by the relation

$$-\tau = \bar{\rho}_M \overline{u'v'} \qquad \text{(B-24)}$$

This equation is the last of the three identifications which are sought.

Summarizing, the mass transfer rate $\dot{m}$, the heat-transfer rate (due to temperature gradient) $\dot{q}$, and the shearing stress τ have been identified with time averages of turbulent fluctuations for the case of unidirectional radial diffusion in the turbulent core of two-component pipe flows with the result

$$\dot{m}_v = \frac{p}{R_v T} \overline{\pi'_v v'} \qquad \text{(B-7)}$$

$$\dot{q} = \bar{\rho}_M \overline{H'_M v'} \qquad \text{(B-16)}$$

$$-\tau = \bar{\rho}_M \overline{u'v'} \qquad \text{(B-24)}$$

As one would expect, the latter two terms are essentially the same as obtain for ordinary turbulent pipe flows with heat transfer but no mass transfer.

NOMENCLATURE

a = velocity of sound

c = mean velocity of molecules

c_p = specific heat at constant pressure

Ca = modified cavitation parameter

C_f = gas-stream friction coefficient

C_h = gas-stream, heat-transfer coefficient

C_m = gas-stream, mass-transfer coefficient

d = duct diameter

D = molecular mass diffusivity

f = evaporation coefficient

g = acceleration of gravity

H = enthalpy

ΔH = coolant heat of vaporization

k = thermal conductivity

L = liquid-film or test-section length

$\dot{m}$ = mass transfer per unit area and per unit time

Ma = Mach number

p = pressure

Pr = Prandtl number

$\dot{q}$ = heat transfer per unit area and per unit time by conduction

r = distance from the center line of the pipe

R = gas constant

Re = Reynolds number

Sc = Schmidt number

t = time

T = temperature

u = velocity in the x direction

$u^* = u/\sqrt{\tau_o/\rho_o}$

v = velocity in the y direction

V = liquid velocity averaged over cross-sectional area of injection orifices

$\dot{w}$ = oxidizer transfer per unit area and per unit time

x = distance along the duct axis

y = distance into gas stream from gas-stream bounding surface measured perpendicularly to bounding surface

$y^* = \rho_o \sqrt{\tau_o/\rho_o}\ y/\mu_o$

γ = specific heat ratio

Γ = liquid flow per unit time and per unit length of tube circumference

δ = gas-stream laminar sublayer thickness

$\delta' = \int_o^\delta (\mu_{M_o}/\mu_M)\, dy$

$\delta^* = \rho_\infty \sqrt{\tau_\delta/\rho_\infty} \int_o^\delta (1/\mu_M) dy$

η = film thickness averaged with respect to x and t

$\eta^* = \rho_{Lf} \sqrt{\tau_o/\rho_{Lf}}\ \eta/\mu_{Lf} \approx \sqrt{2\Gamma/\mu_{Lf}}$

θ = oxidizer specific concentration (weight of oxidizer per unit total weight)

μ = dynamic viscosity

π = 3.14

$\pi_k = p_k/p$

ρ = density

τ = shearing stress

$\underline{\Phi}$ = viscous dissipation terms in general energy equation

Subscripts

G = gas

k = summation index

Lf = liquid in the film

Li = liquid in the injector orifice

M = mixture of gas and vapor

s = saturation conditions corresponding to T_o

t = total

V = vapor

o = bounding surface of gas stream (a liquid film surface or a duct wall)

δ = junction of turbulent core and laminar sublayer in gas stream

∞ = bulk property or average velocity

TABLE I

DATA FROM TESTS MADE FOR PURPOSE OF DETERMINING PROTECTED SURFACE AREA VS COOLANT-FLOW RATE IN 2.90-INCH ID FILM-COOLED CIRCULAR DUCT

Test Number	Water-Flow Rate (lb/sec)	Protected-Surface Area (sq. in.)	Pressure Drop[a] (in. Water)
Air-Flow Rate = 1.70 lb/sec; Static Pressure = 15.7 psia; Bulk Temp. = 1103°R			
20	0.0617	523.5	32.2
21	0.0506	454.5	36.0
22	0.0444	424.7	39.8
23	0.0425	424.1	41.6
24	0.0361	371.7	44.3
25	0.0303	321.4	47.1
26	0.0244	280.1	47.3
27	0.0217	231.9	48.6
28	0.0172	138.5	49.7
29	0.0117	67.2	-
30	0.0092	49.6	-
Air-Flow Rate = 1.65 lb/sec; Static Pressure = 16.7 psia; Bulk Temp. = 1499°R			(psi)
31	0.130	411.6	1.8
32	0.122	394.7	2.0
33	0.110	365.9	2.2
34	0.104	350.7	2.3
35	0.0944	331.5	2.4
36	0.0867	315.4	2.7
37	0.0772	290.0	2.9
38	0.0680	272.5	3.0
39	0.0583	225.0	3.1
40	0.0492	187.5	3.1
41	0.0397	186.6	3.2
42	0.0328	88.2	3.1
43	0.0222	60.3	3.1
44	0.0139	45.1	3.2

[a] "Pressure drop" is the pressure differential between stations P_4 and P_5; cf. Figure 2.

TABLE I (Cont'd)

Test Number	Water-Flow Rate (lb/sec)	Protected-Surface Area (sq. in.)	Pressure Drop (in. Water)
Air-Flow Rate = 0.86 lb/sec; Static Pressure = 14.6 psia; Bulk Temp. = 1621°R			
			(in. Water)
45	0.0522	486.8	11.3
46	0.0475	457.5	11.7
47	0.0417	419.1	12.1
48	0.0383	404.5	12.3
49	0.0339	360.5	12.6
50	0.0272	277.4	13.1
51	0.0233	248.2	13.4
52	0.0194	199.0	13.8
53	0.0133	57.6	14.3
54	0.0097	49.0	14.6
Air-Flow Rate = 0.85 lb/sec; Static Pressure = 14.7 psia; Bulk Temp. = 1584°R			
61	0.0492	501.4	13.0
62	0.0444	449.2	13.0
63	0.0378	415.9	13.3
64	0.0322	360.8	13.7
65	0.0267	270.8	14.1
66	0.0228	218.9	14.4
67	0.0172	98.8	14.7
68	0.0108	46.3	15.0
Air-Flow Rate = 0.65 lb/sec; Static Pressure = 14.4 psia; Bulk Temp. = 2214°R			
89	0.0617	523.0	9.0
90	0.0553	486.4	8.7
91	0.0492	432.4	8.7
92	0.0439	427.0	8.7
93	0.0375	353.6	8.7
94	0.0326	307.2	8.8
95	0.0276	248.4	9.0
96	0.0226	195.0	9.0
97	0.0171	88.7	8.9
98	0.0136	49.3	8.8
99	0.0094	42.2	8.8
Air-Flow Rate = 0.43 lb/sec; Static Pressure = 14.2 psia; Bulk Temp. = 2239°R			
100	0.0294	350.0	3.6
101	0.0264	321.6	3.9

TABLE I (Cont'd)

Test Number	Water-Flow Rate (lb/sec)	Protected-Surface Area (sq. in.)	Pressure Drop (in. Water)
102	0.0225	258.7	4.0
103	0.0193	224.6	4.0
104	0.0160	137.9	4.0
105	0.0126	50.0	4.0
106	0.0092	48.4	4.0
Air-Flow Rate = 1.54 lb/sec; Static Pressure = 15.8 psia; Bulk Temp. = 1514°R			
107	0.151	499.9	28.7
108	0.135	465.0	32.5
109	0.127	453.2	34.6
110	0.116	425.1	37.0
111	0.107	405.4	39.0
112	0.0912	365.0	42.5
113	0.0803	--	44.5
114	0.0679	297.3	47.0
115	0.0585	270.7	48.5
116	0.0417	205.3	--
117	0.0348	151.4	--
118	0.0247	41.7	--

TABLE II

CALCULATION SHEET FOR PARAMETER VALUES AT INCEPTION POINT OF UNSTABLE LIQUID-FILM FLOW (GAS = UNHEATED AIR)

Study Medium	Test Number	Liquid	Experimental Data: Static Pressure p (psia)	Experimental Data: Liquid Flow Γ (lb/ft sec) x 10^2	Experimental Data: Film Temp. T_o (^oR)	Calculated Parameters: Air Viscosity μ_{M_o} (lb/ft sec) x 10^5	Calculated Parameters: Liquid Viscosity μ_{Lf} (lb/ft sec) x 10^4	Calculated Parameters: Viscosity Ratio μ_{M_o}/μ_{Lf} x 10^2	Calculated Parameters: Film Thickness η^*
Motion pictures	123	water	14.1	3.1	526	1.22	6.9	1.76	9.4
Spark photos	203	"	14.2	3.3	515	1.20	8.2	1.46	8.9
Visual observ.	210	"	14.1	2.6	510	1.19	8.8	1.35	7.7
"	211	"	14.1	2.6	511	1.19	8.7	1.37	7.8
"	212	"	28.9	2.4	512	1.19	8.6	1.40	7.5
"	217	22.8°/o sucrose	14.2	2.5	514	1.20	19.1	0.63	5.2
"	218	27.6°/o sucrose	14.2	2.2	516	1.19	23.0	0.52	4.4
"	Ref. 6 Table I	water	25	3.8	510	1.19	8.8	1.35	9.3

TABLE III

CALCULATION SHEET FOR PARAMETER VALUES AT INCEPTION POINT OF UNSTABLE LIQUID-FILM FLOW (WITH HEATED GASES)

	Experimental Data			Calculated Parameters				
Data Source	Static Pressure p (psia)	Liquid Flow Γ (lb/ft sec)	Gas Bulk Temp. T_∞ (^oR)	Film Temp. T_o (^oR)	Mixture Viscosity μ_{M_o} (lb/ft sec) x 10^5	Liquid Viscosity μ_{Lf} (lb/ft sec) x 10^4	Viscosity Ratio μ_{M_o}/μ_{Lf} x 10^2	Film Thickness η^+
This paper	15.7	0.044	1103	595	1.25	3.26	3.84	16.5
This paper	16.7	0.065	1499	613	1.23	2.80	4.39	21.6
This paper	14.6	0.049	1621	617	1.21	2.72	4.45	19.0
This paper	14.7	0.047	1584	616	1.21	2.75	4.40	18.5
This paper	14.4	0.055	2214	630	1.16	2.47	4.70	21.2
This paper	15.8	0.065	1514	614	1.23	2.79	4.41	21.6
Ref. 11 Fig. 4	25[a]	0.056	1360	629	1.26	2.50	5.04	21.2
"	"	0.074	1360	629	1.26	2.50	5.04	24.4
"	"	0.063	1360	629	1.26	2.50	5.04	22.5
"	"	0.092	1860	646	1.23	2.23	5.52	28.8
"	"	0.101	2060	650	1.22	2.16	5.65	30.6
"	"	0.082	1460	634	1.26	2.40	5.25	26.2
"	"	0.083	1660	641	1.25	2.30	5.43	26.8
"	"	0.086	2060	650	1.22	2.16	5.65	28.2
"	"	0.066	1260	624	1.27	2.59	4.91	22.6
"	"	0.070	1260	624	1.27	2.59	4.91	23.2

[a] Based on boiling point given in Ref. 11

TABLE IV

CALCULATION SHEET FOR MASS-FLOW RATIOS

(Test Conditions Correspond to Inception Point of Unstable Flow; Gas = Air; Liquid = Water)

Data Source	Gas Bulk Temp. T_∞ ($^\circ$R)	Gas Reynolds Number Re_G x 10^{-5}	Friction Coefficient[a] C_f x 10^3	Theoretical $\frac{\dot{m}_e}{\rho_\infty u_\infty}$ x 10^4	Duct Diameter d (in.)	Liquid-Film Length L (in.)	Entrance-Condition Correction[b]	Corrected $\frac{\dot{m}_e}{\rho_\infty u_\infty}$ x 10^4	Experimental $\frac{\dot{m}_e}{\rho_\infty u_\infty}$ x 10^4
This paper	1103	4.33	3.4	2.0	2.90	39.6	1.63	3.3	3.6
" "	1499	3.41	3.5	3.8	2.90	25.5	1.92	7.3	8.5
" "	1621	1.69	4.0	4.9	2.90	42.8	1.46	7.2	7.3
" "	1584	1.69	4.0	4.8	2.90	45.0	1.44	6.9	6.8
" "	2214	1.05	4.4	8.7	2.90	44.0	1.39	12.1	10.6
" "	1514	3.17	3.6	3.9	2.90	27.0	1.85	7.2	8.6
Ref. 11 Fig. 4	1360	8.18	3.0	2.7	4.00	19.2	3.09	8.3	6.0
"	1360	9.90	2.9	2.6	4.00	19.7	3.14	8.2	6.4
"	1360	6.00	3.2	2.8	4.00	30.6	2.21	6.2	5.8
"	1860	5.25	3.2	4.9	4.00	19.0	2.89	14.2	12.9
"	2060	4.70	3.3	5.8	4.00	18.0	2.94	17.0	14.9
"	1460	4.93	3.3	3.3	2.00	18.4	1.96	6.5	7.3
"	1660	3.47	3.5	4.4	2.00	20.6	1.79	7.9	8.6
"	2060	2.51	3.7	6.6	2.00	17.5	1.85	12.2	12.5
"	1260	4.42	3.4	2.6	2.00	30.0	1.57	4.1	4.4
"	1260	5.64	3.2	2.5	2.00	21.6	1.85	4.4	5.1

[a] Friction coefficients are taken to be those corresponding to ordinary turbulent flows in smooth pipes.

[b] Entrance-condition correction in this case is $1 + (1/3)Re_G^{1/4}\,(d/L)$.

TABLE V

DATA FROM TESTS MADE FOR PURPOSE OF DETERMINING WALL TEMPERATURE OF FILM-COOLED DUCT

(Gas = Air; Coolant = Water; Duct Diameter = 2.90 Inches)

Test Number	Gas-Stream Bulk Temp. (^{o}R)	Test-Section Static Pressure (psia)	Minimum Wall Temp. (^{o}R)
20	1103	15.7	595
31	1499	16.7	616
45	1621	14.6	620
55	1453	14.5	607
56	1634	14.6	620
57	1786	14.7	625
58	1972	14.8	629
59	2118	15.0	633
60	2277	15.2	637
61	1584	14.7	616
89	2214	14.4	629
100	2239	14.2	629
107	1514	15.8	612

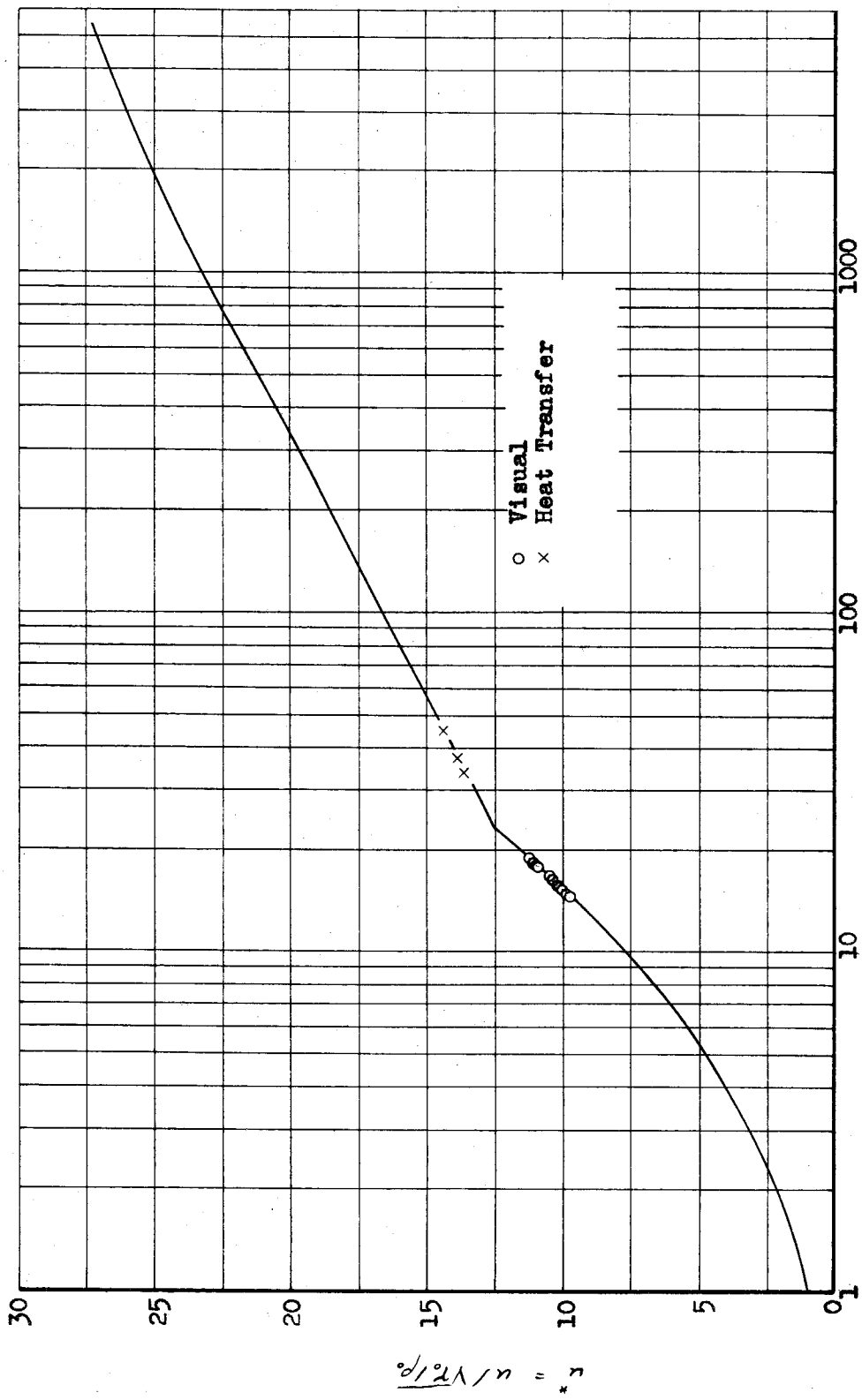

Figure 1. Association of Visual-Flow Regions and Heat-Transfer Results with Generalized Velocity Distribution for Fully Developed Flow in Smooth Tubes Applied to Liquid Films (from Fig. 6 of Ref. 6)

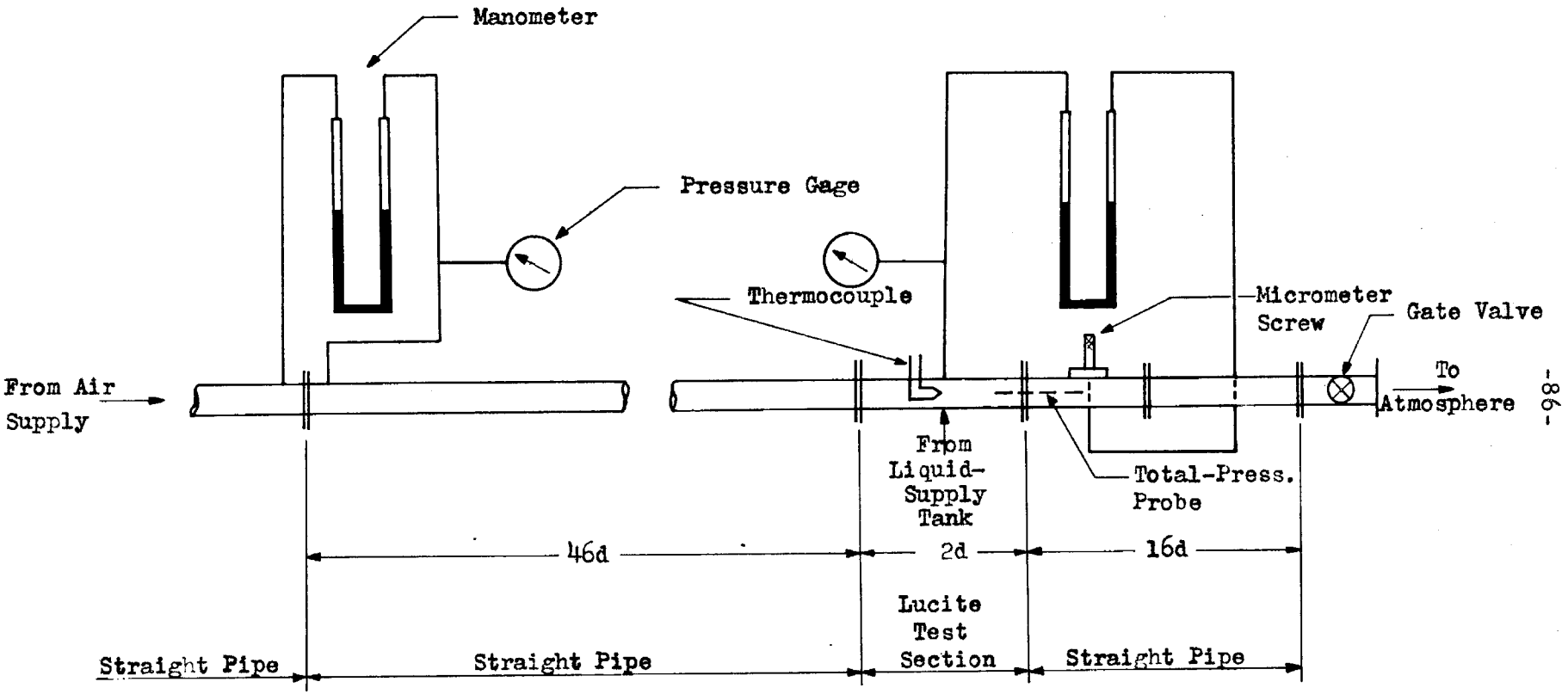

Figure 2. Flow Diagram for Equipment Used in Research on Attachment of Liquid Wall Films

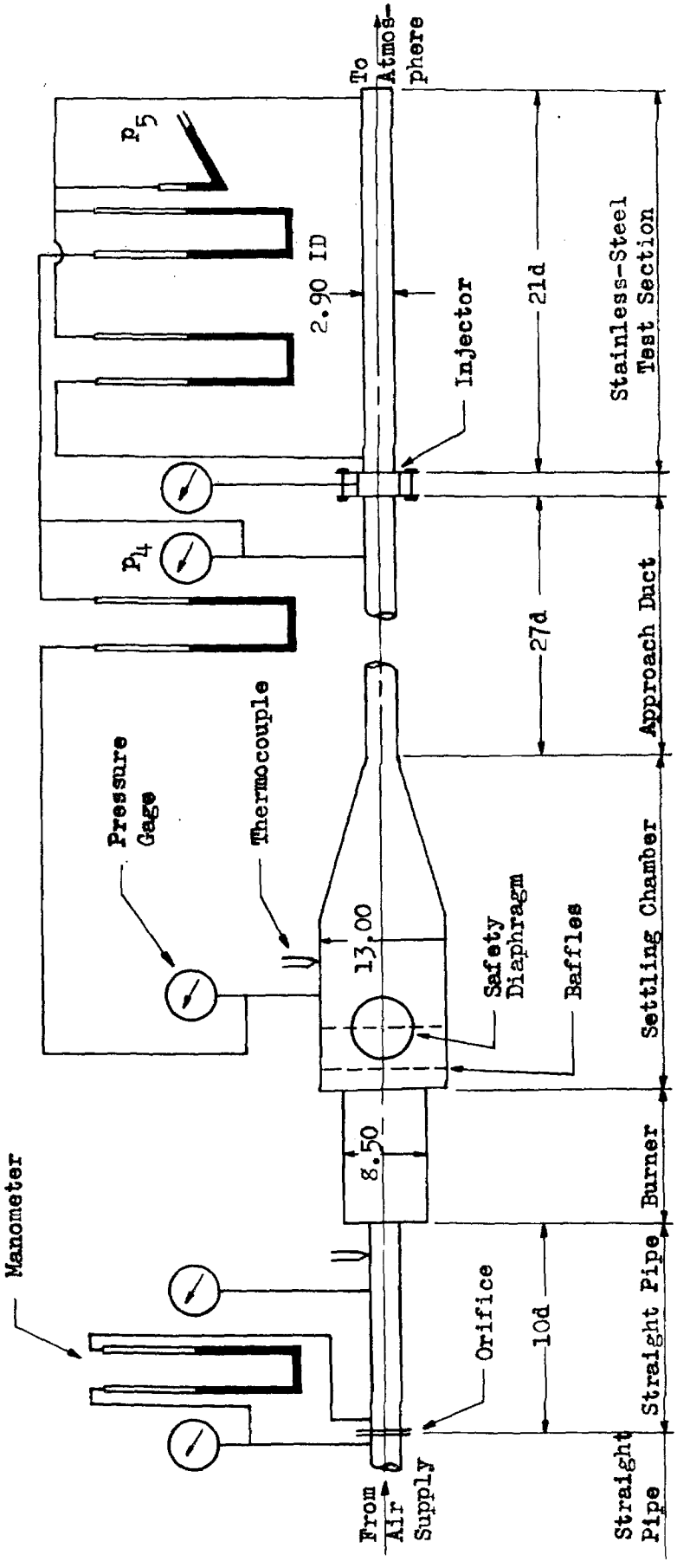

Figure 3. Flow Diagram for Equipment Used in Research on Stability of and Evaporation from Liquid Wall Films

Figure 4. Exploded Views of Coolant Injector Used in Research on Liquid Wall Films

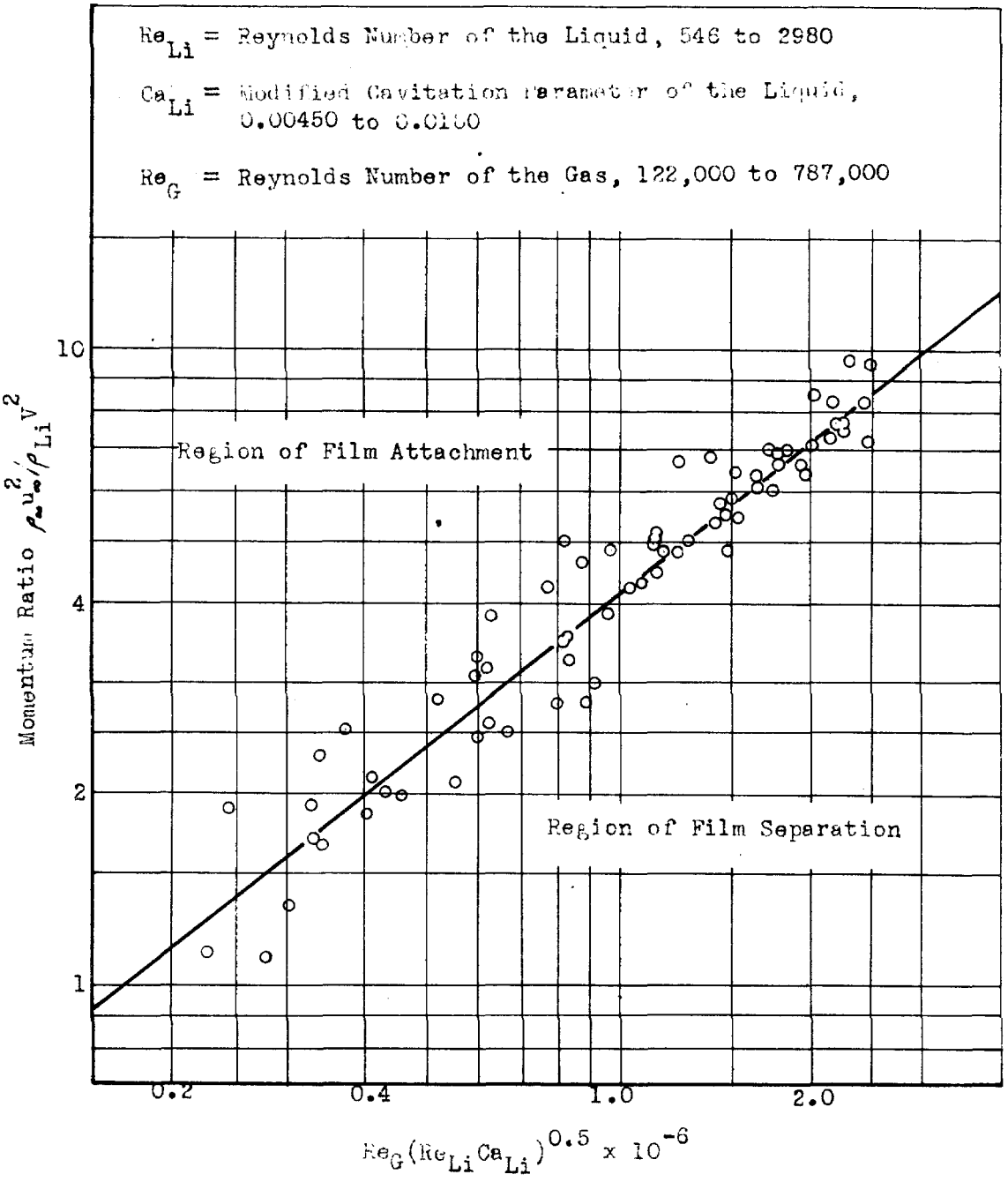

Figure 5. Dimensionless Plot of Film-Attachment Data Taken at Critical Velocity of Injection

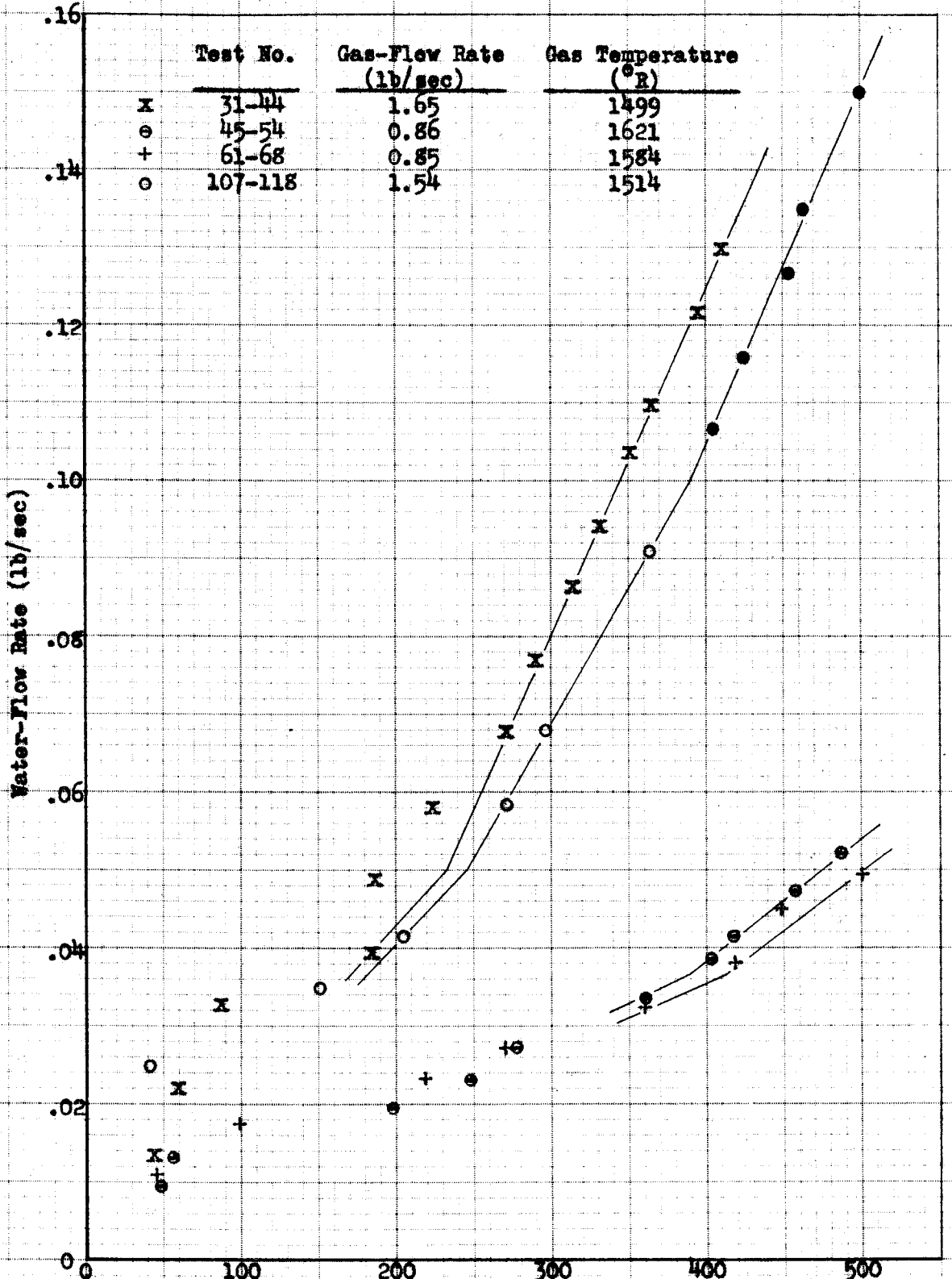

Figure 6. Water-Flow Rate vs Area of Protected Surface for Several Gas-Flow Rates

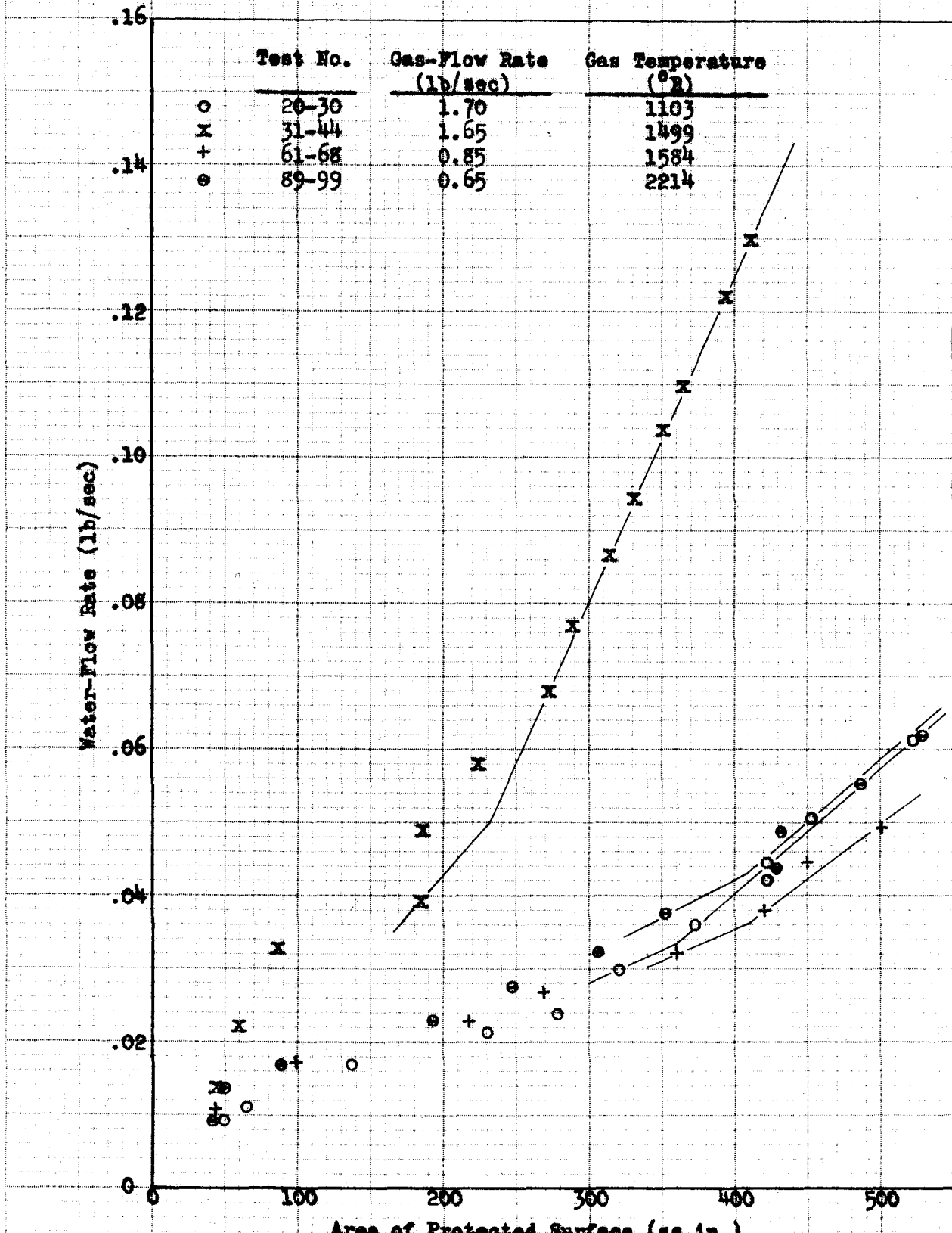

Figure 7. Water-Flow Rate vs Area of Protected Surface for Several Gas Temperatures

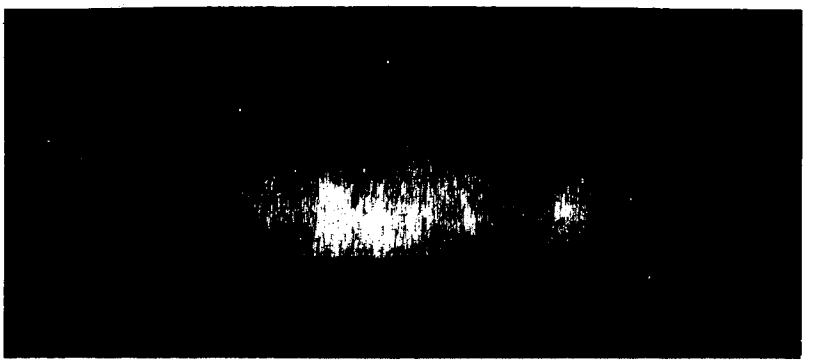

Dimensionless Film Thickness $\eta^* = 7.1$

Dimensionless Film Thickness $\eta^* = 9.2$

Figure 8a: Representative Spark Photographs of Annular Two-Phase Adiabatic Flow in 3-Inch ID Lucite Duct (Gas = Air; Liquid = Water; Gas-Stream Reynolds Number = 452,000)

Dimensionless Film Thickness $\eta^* = 12.0$

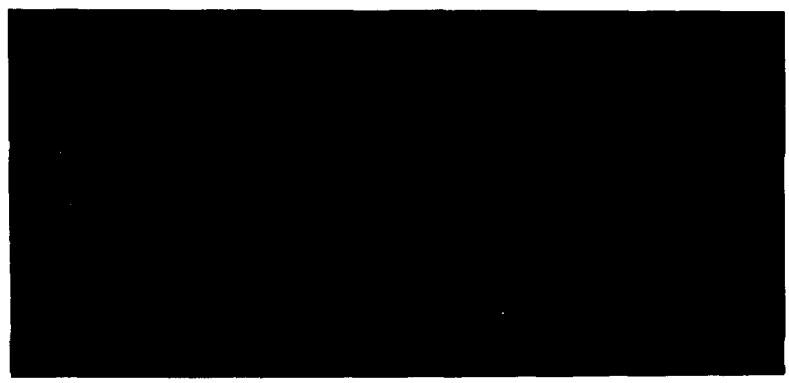

Dimensionless Film Thickness $\eta^* = 15.2$

Figure 8b: Representative Spark Photographs of Annular Two-Phase Adiabatic Flow in 3-Inch ID Lucite Duct (Gas = Air; Liquid = Water; Gas-Stream Reynolds Number = 452,000)

Gas-Stream Reynolds Number, 282,000

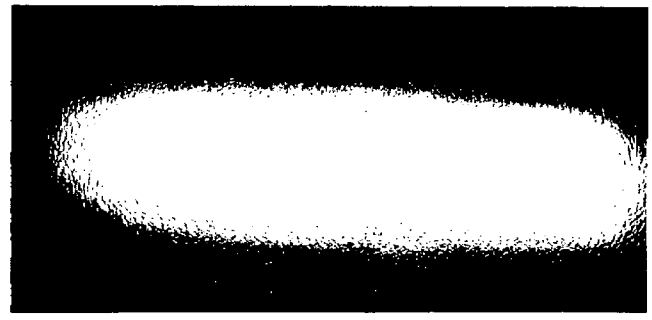

Gas-Stream Reynolds Number, 503,000

Figure 9: Representative Spark Photographs of Annular Two-Phase Adiabatic Flow in 3-Inch ID Lucite Duct (Gas = Air; Liquid = Water; Dimensionless Film Thickness $\eta^* = 7.6$)

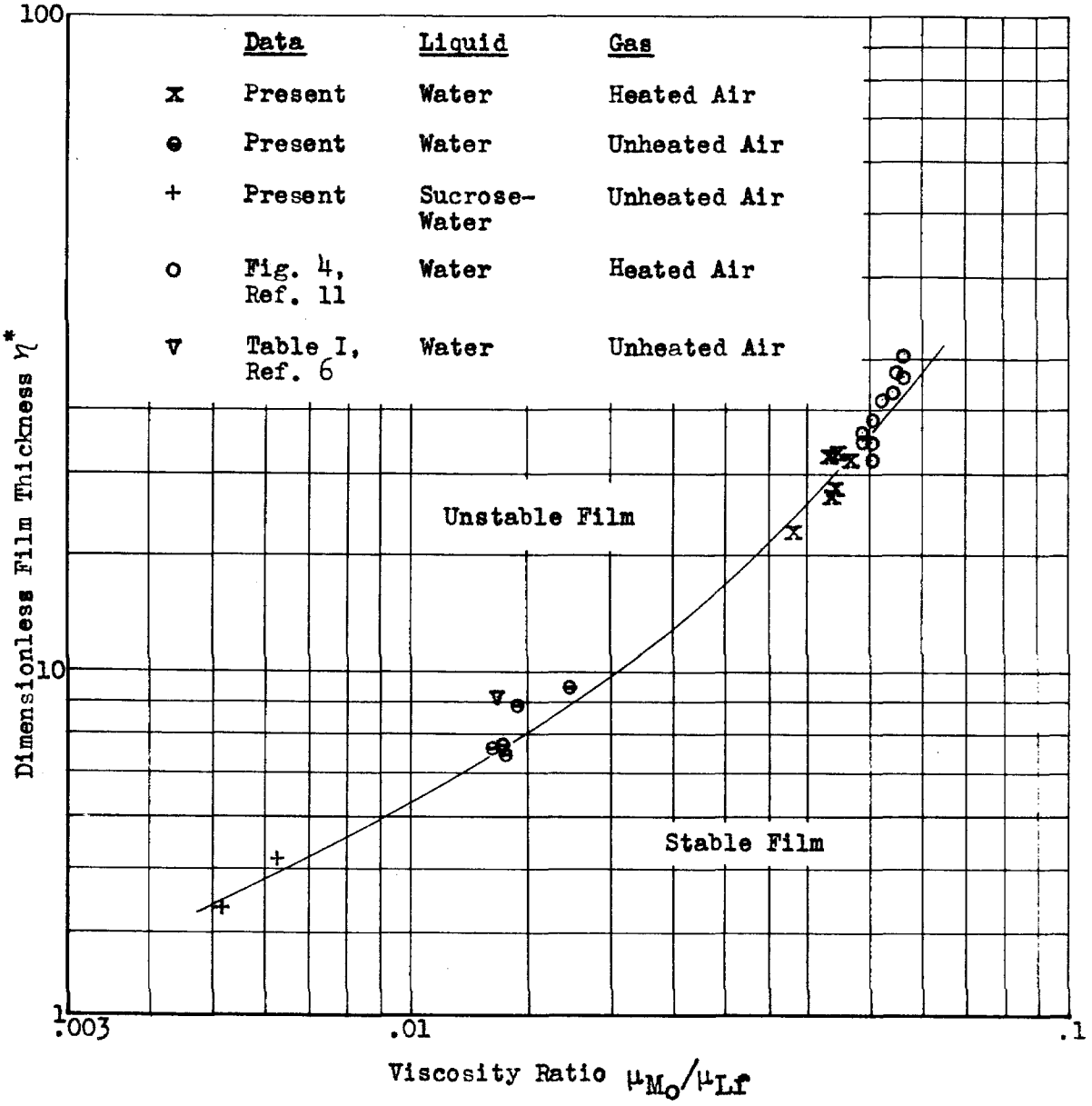

Figure 10. Dimensionless Film Thickness vs Ratio of Viscosity of Gas-Vapor Mixture to That of Liquid at Inception Point of Long-Wavelength Disturbances

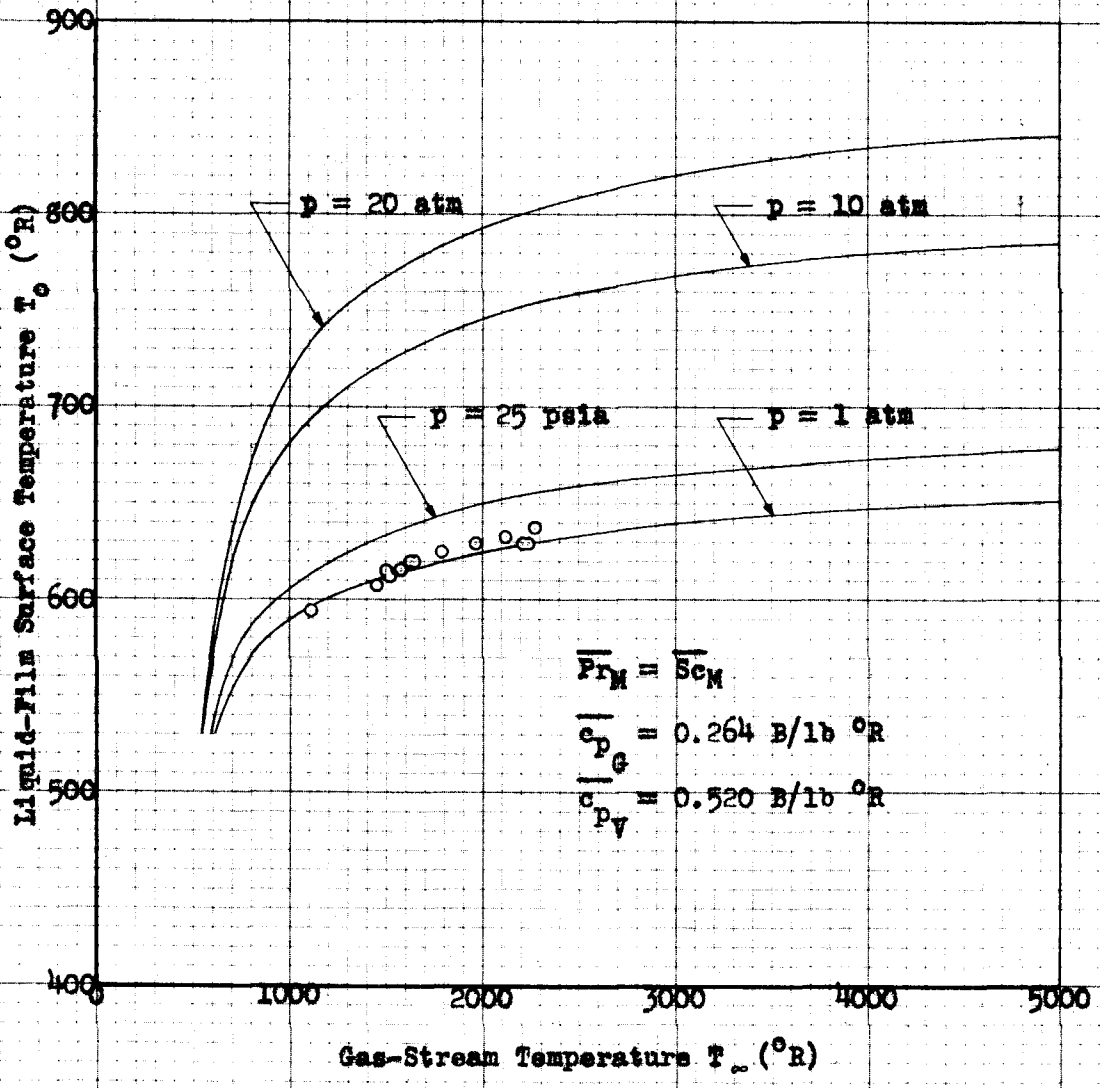

Figure 11. Liquid-Film Surface Temperature vs Gas-Stream Temperature for Water Film Flowing Under Influence of Fully Developed Turbulent Hot-Air Stream in Duct

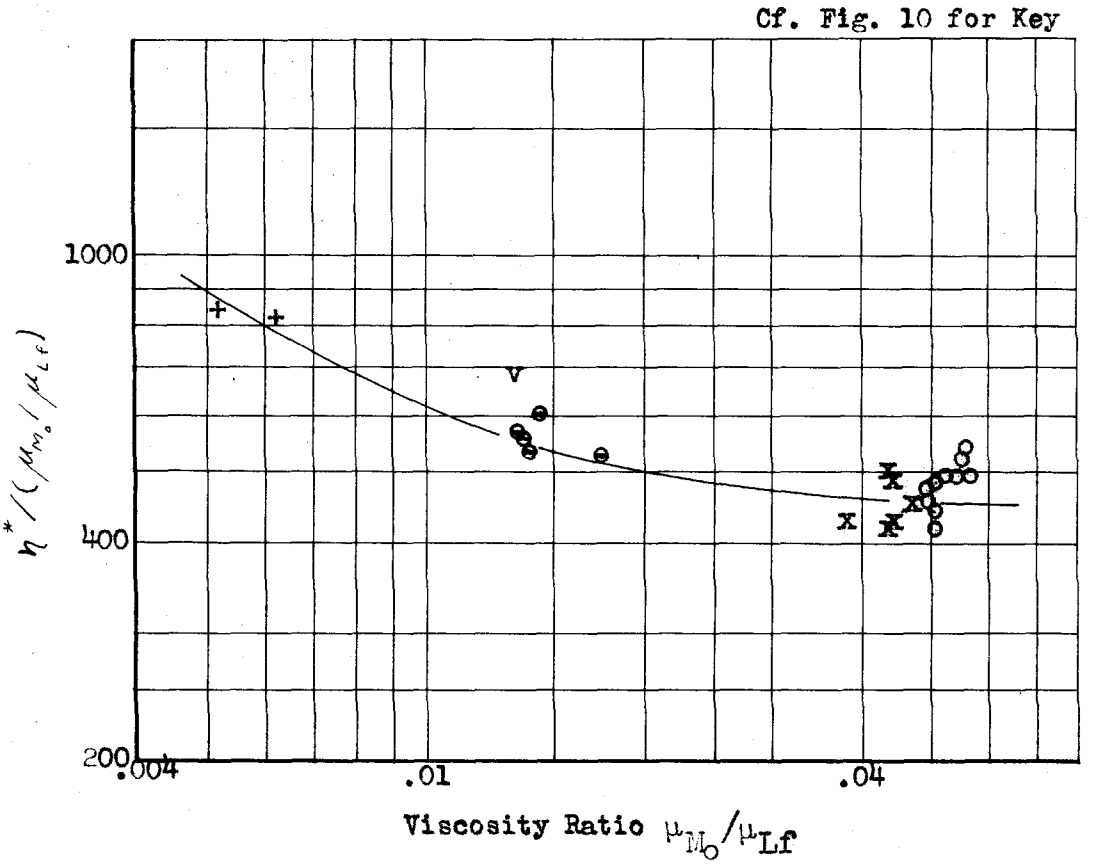

Figure 12. Dimensionless Film Thickness η^* Divided by μ_{M_o}/μ_{Lf} ($= \rho_{Lf}\sqrt{\tau_o/\rho_{Lf}}\,\eta/\mu_{M_o}$) vs μ_{M_o}/μ_{Lf} at Inception Point of Long-Wavelength Disturbances

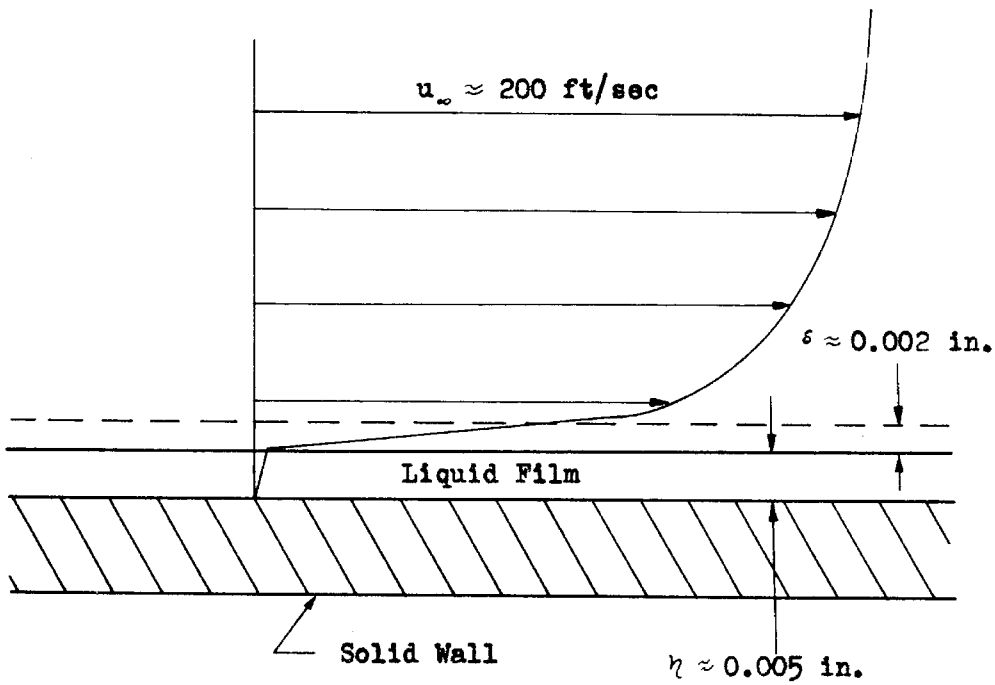

Liquid-Film Surface Velocity $u_0 \approx 3$ ft/sec

Characteristic Length of Small Disturbances ≈ 0.1 in.

Figure 13. Velocity Diagram for Typical Stable Liquid Wall Film Flowing Under Influence of Turbulent Gas Stream

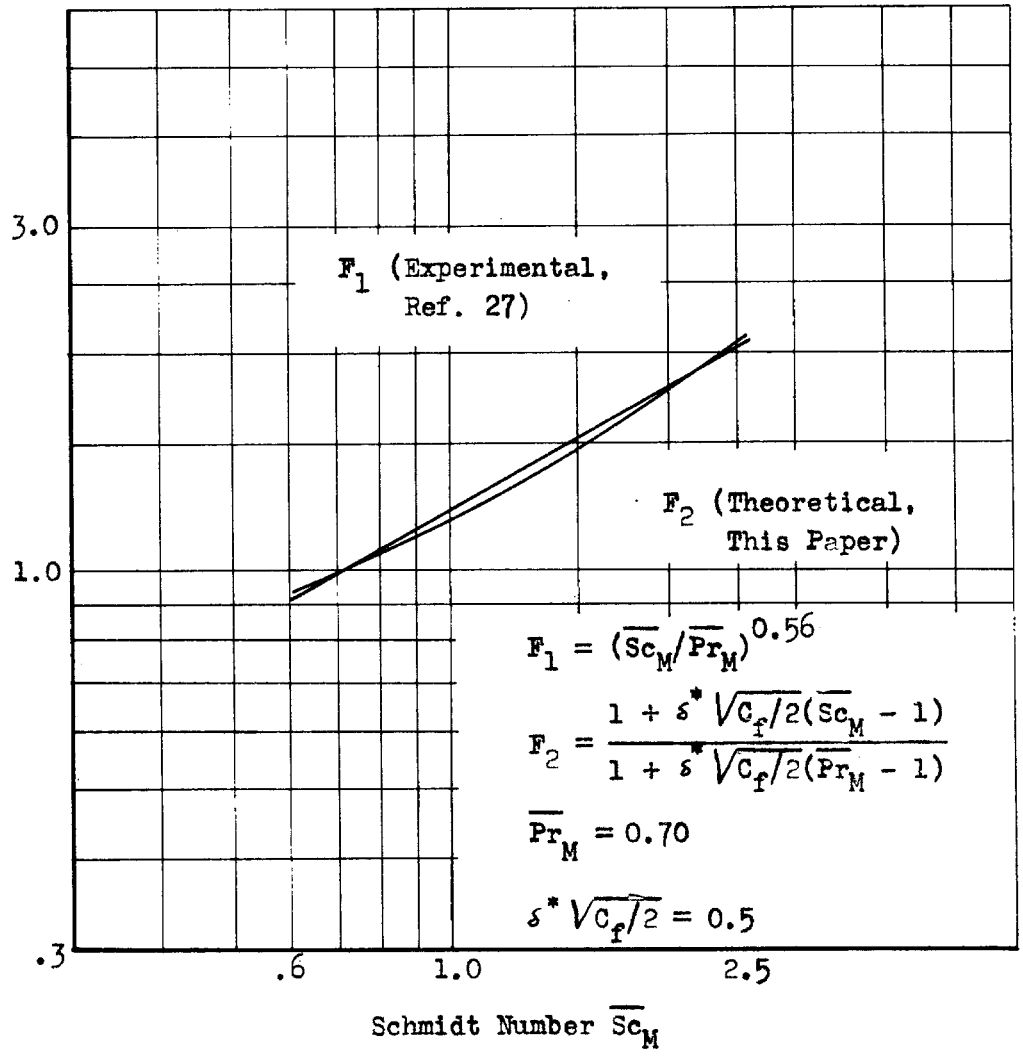

Figure 14. Comparison of Experimental with Theoretical Function of $\overline{Sc}_M$ and $\overline{Pr}_M$ Which Appears in Wet-Bulb-Thermometer Equation

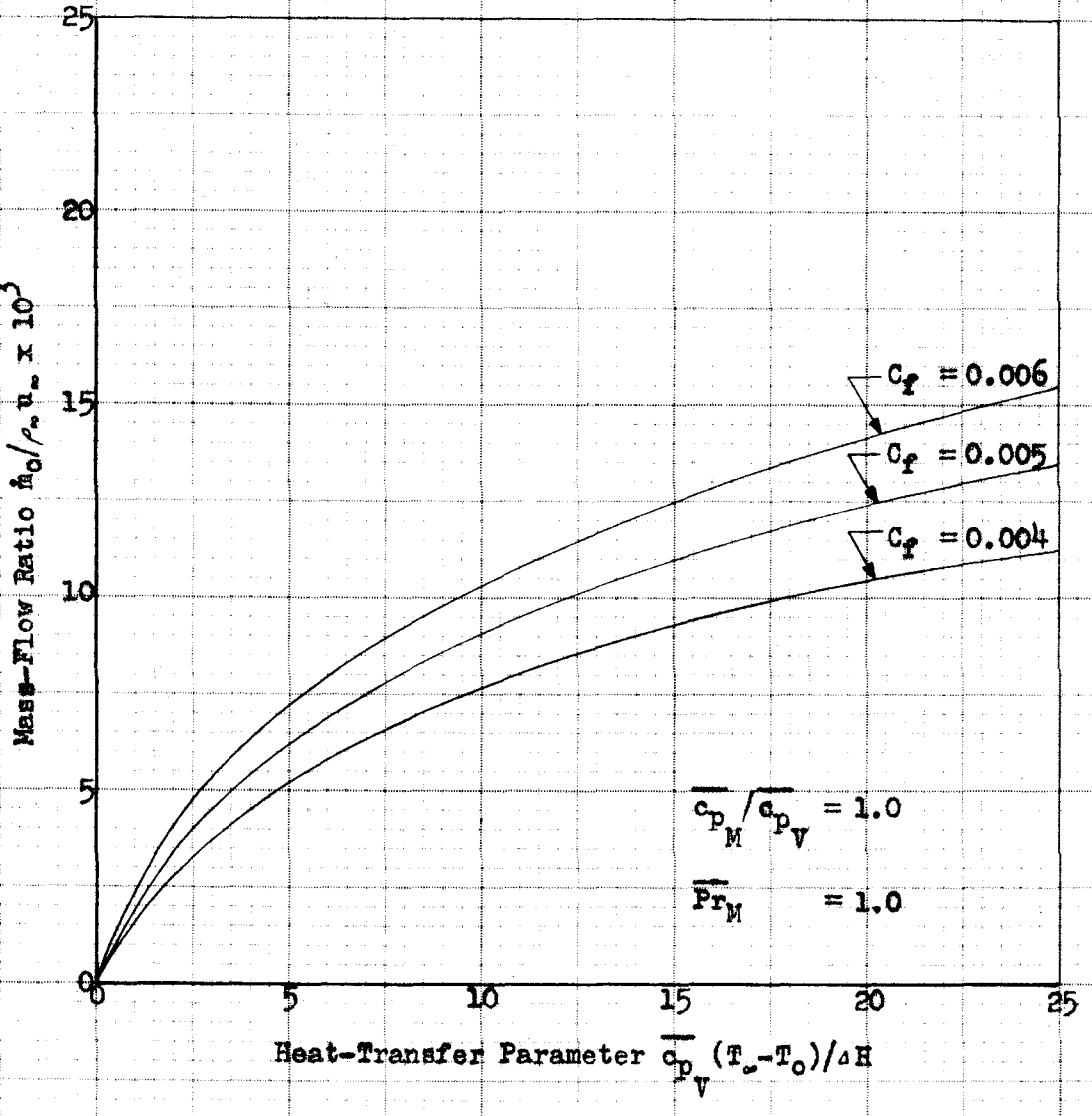

Figure 15a. Mass-Flow Ratio vs Heat-Transfer Parameter for Several Values of C_f

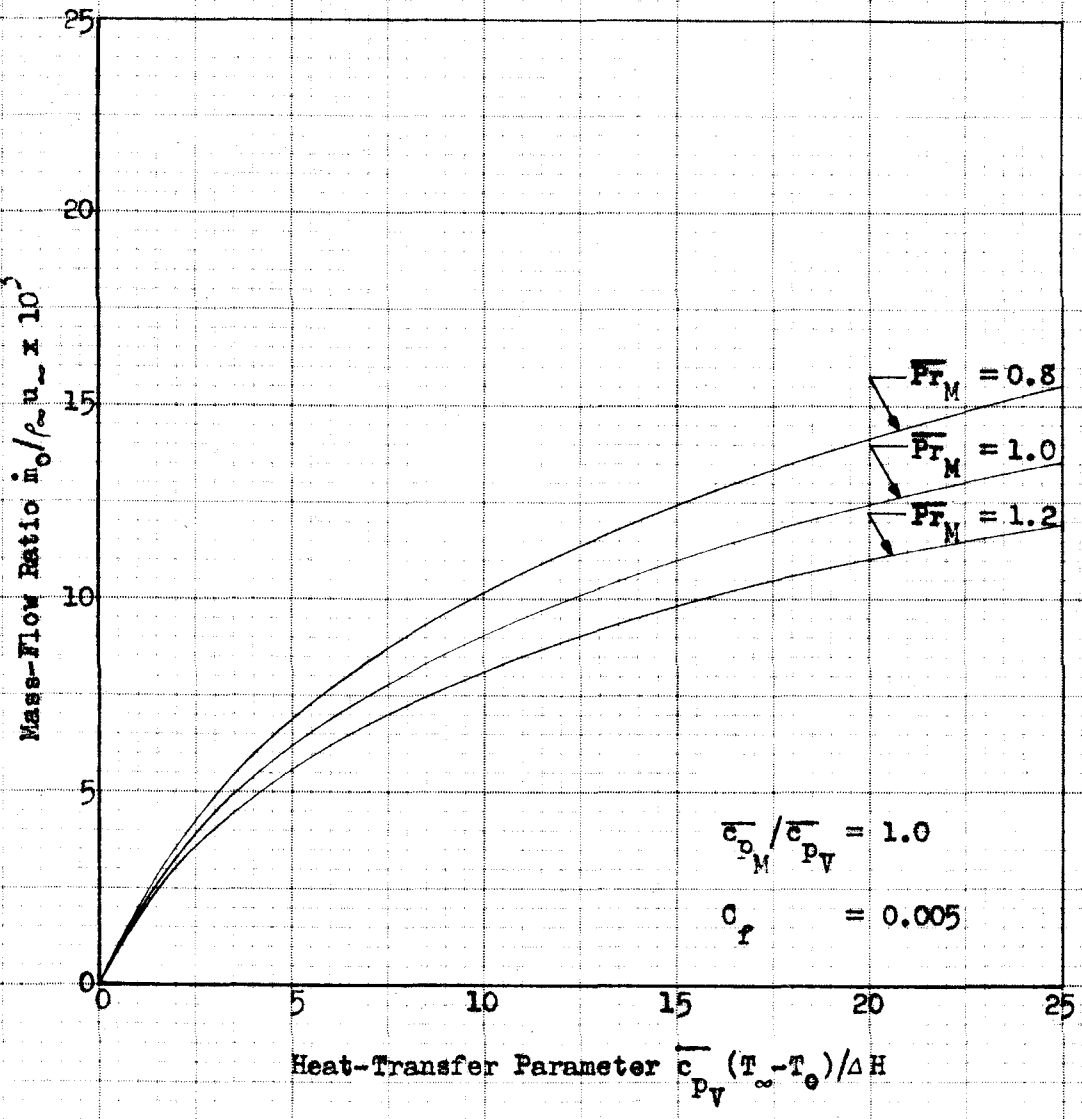

Figure 15b. Mass-Flow Ratio vs Heat-Transfer Parameter for Several Values of $\overline{Pr}_M$

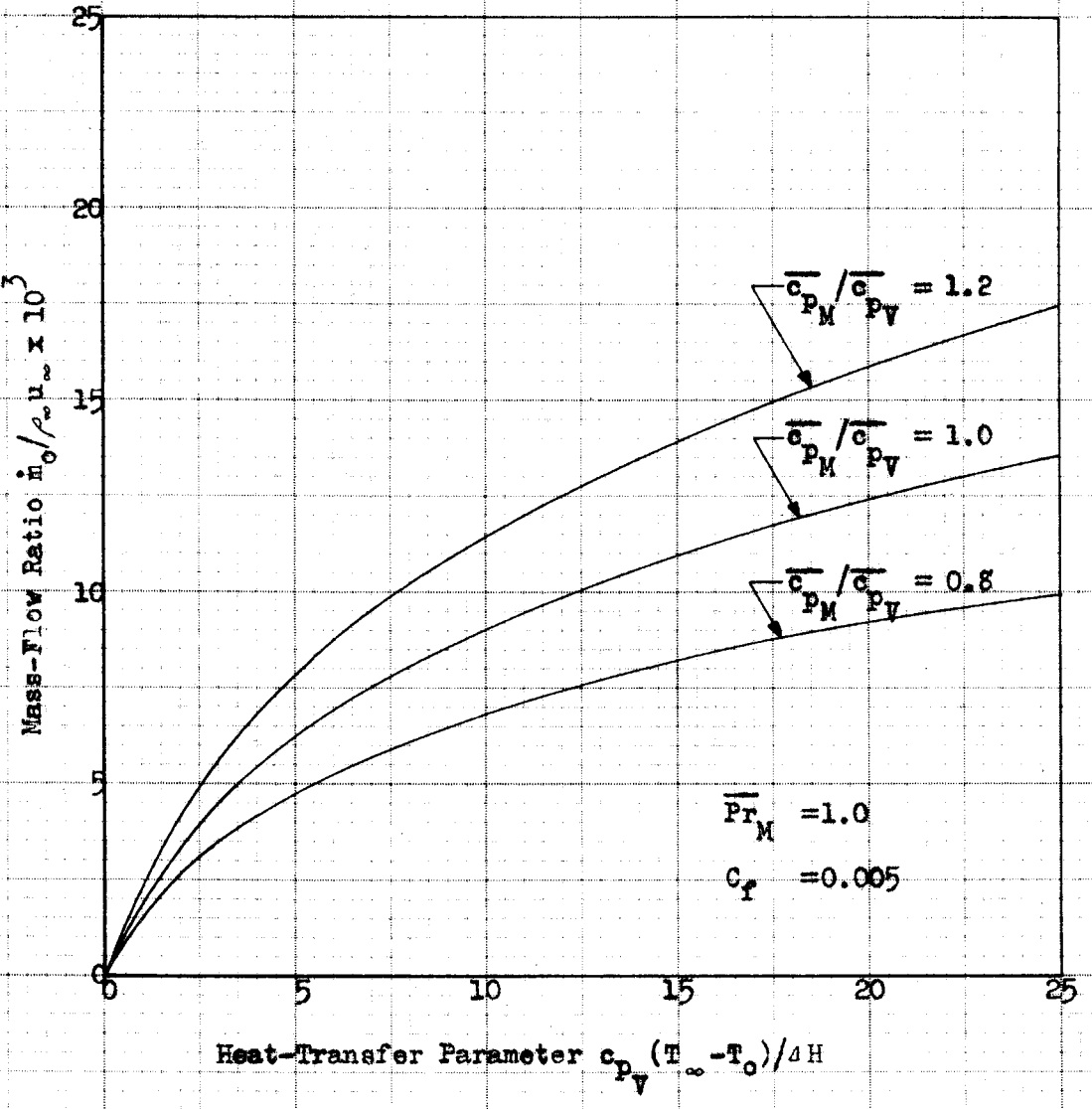

Figure 15c. Mass-Flow Ratio vs Heat-Transfer Parameter for Several Values of $\overline{c_{p_M}}/\overline{c_{p_V}}$

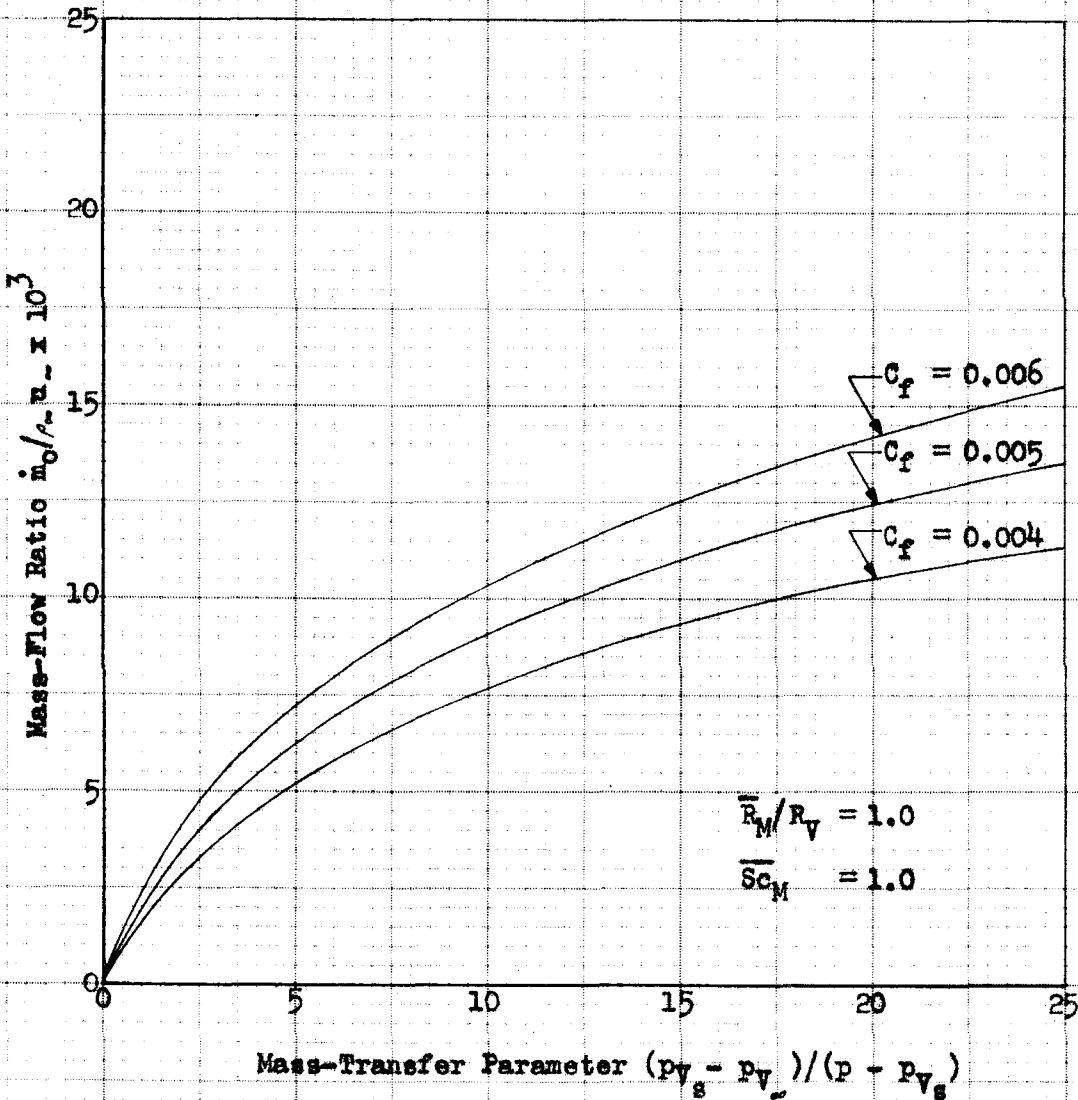

Figure 16a. Mass-Flow Ratio vs Mass-Transfer Parameter for Several Values of C_f

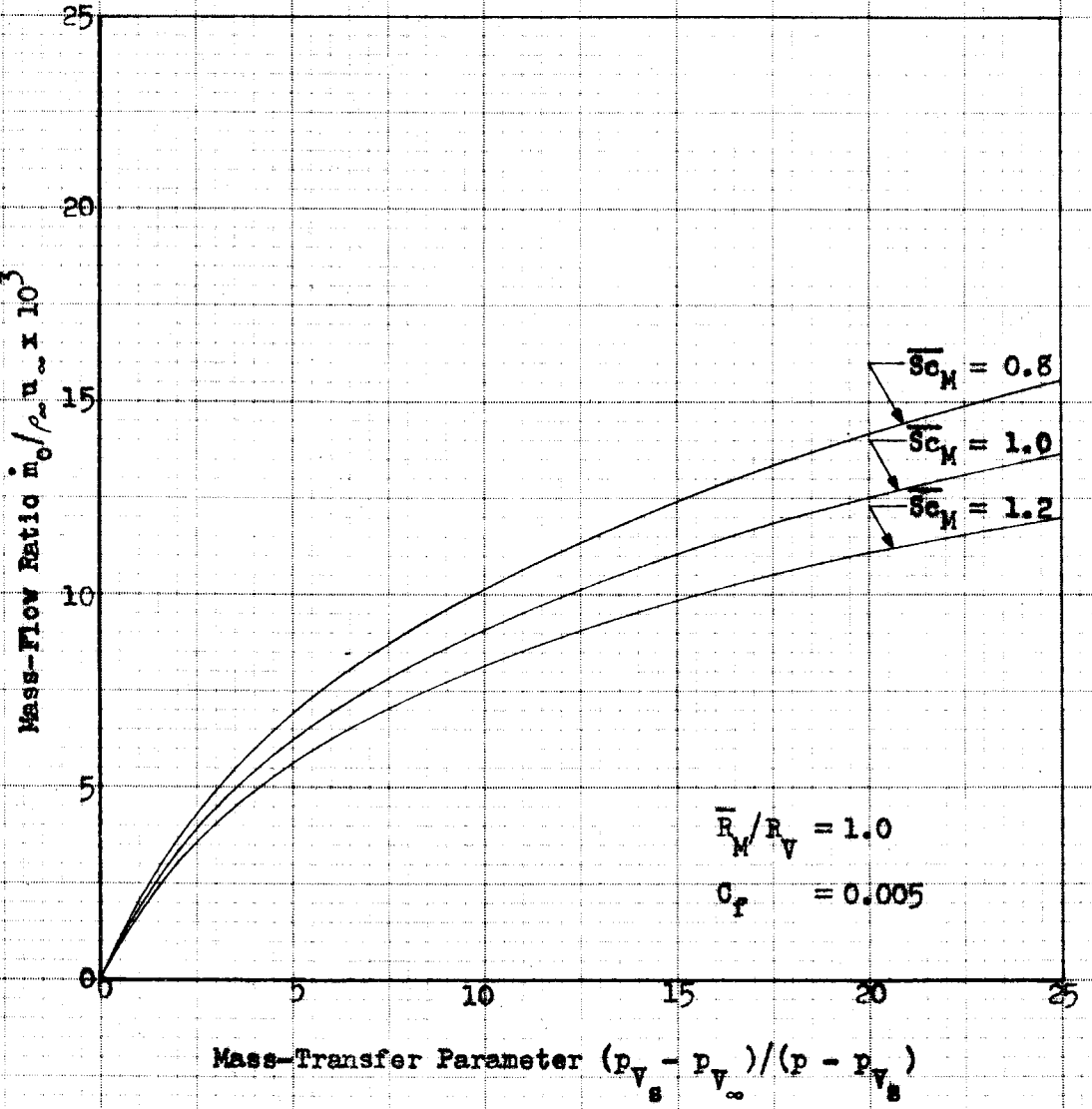

Figure 16b. Mass-Flow Ratio vs Mass-Transfer Parameter for Several Values of $\overline{Sc}_M$

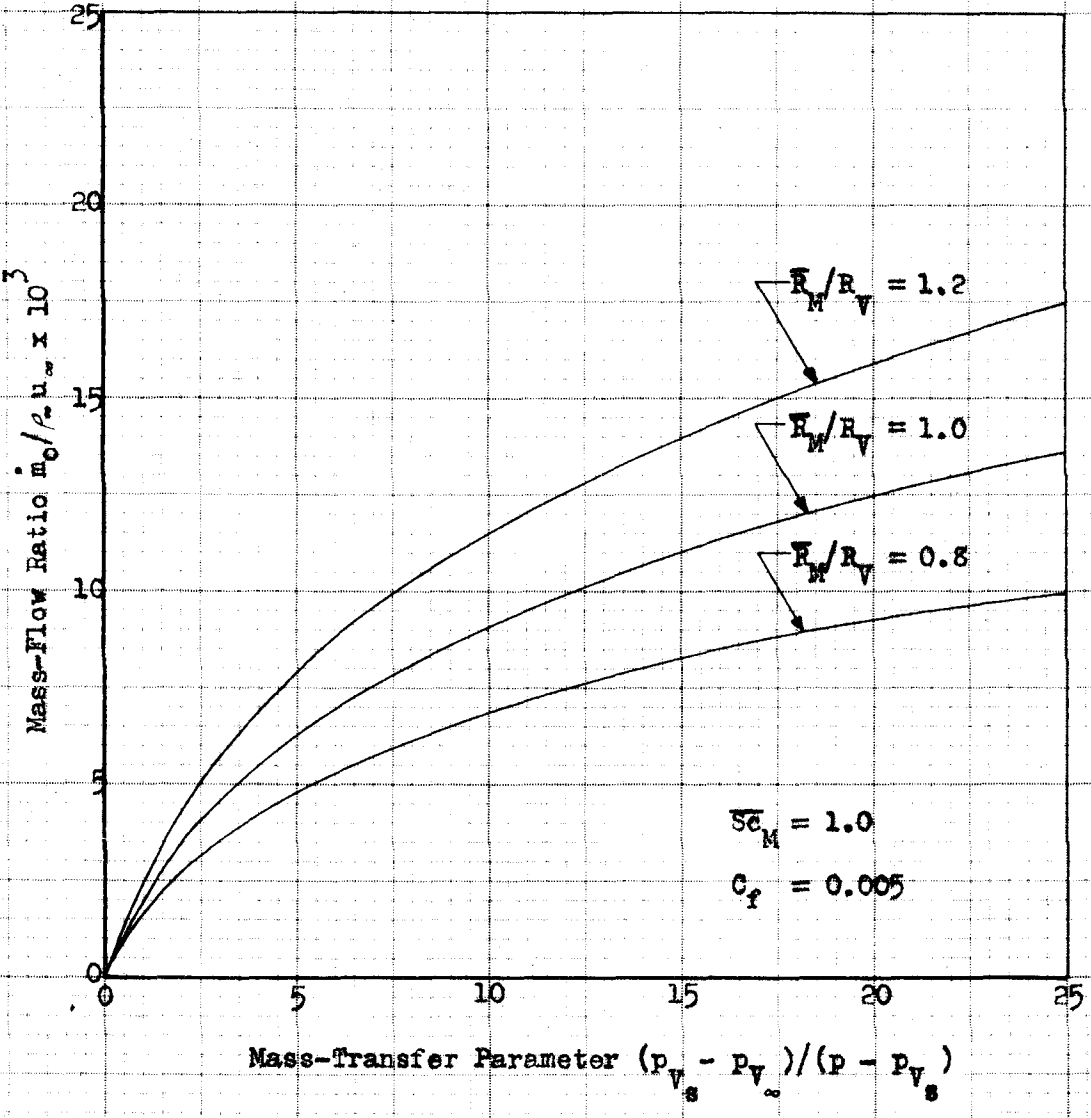

Figure 16c. Mass-Flow Ratio vs Mass-Transfer Parameter for Several Values of $\overline{R}_M/R_V$

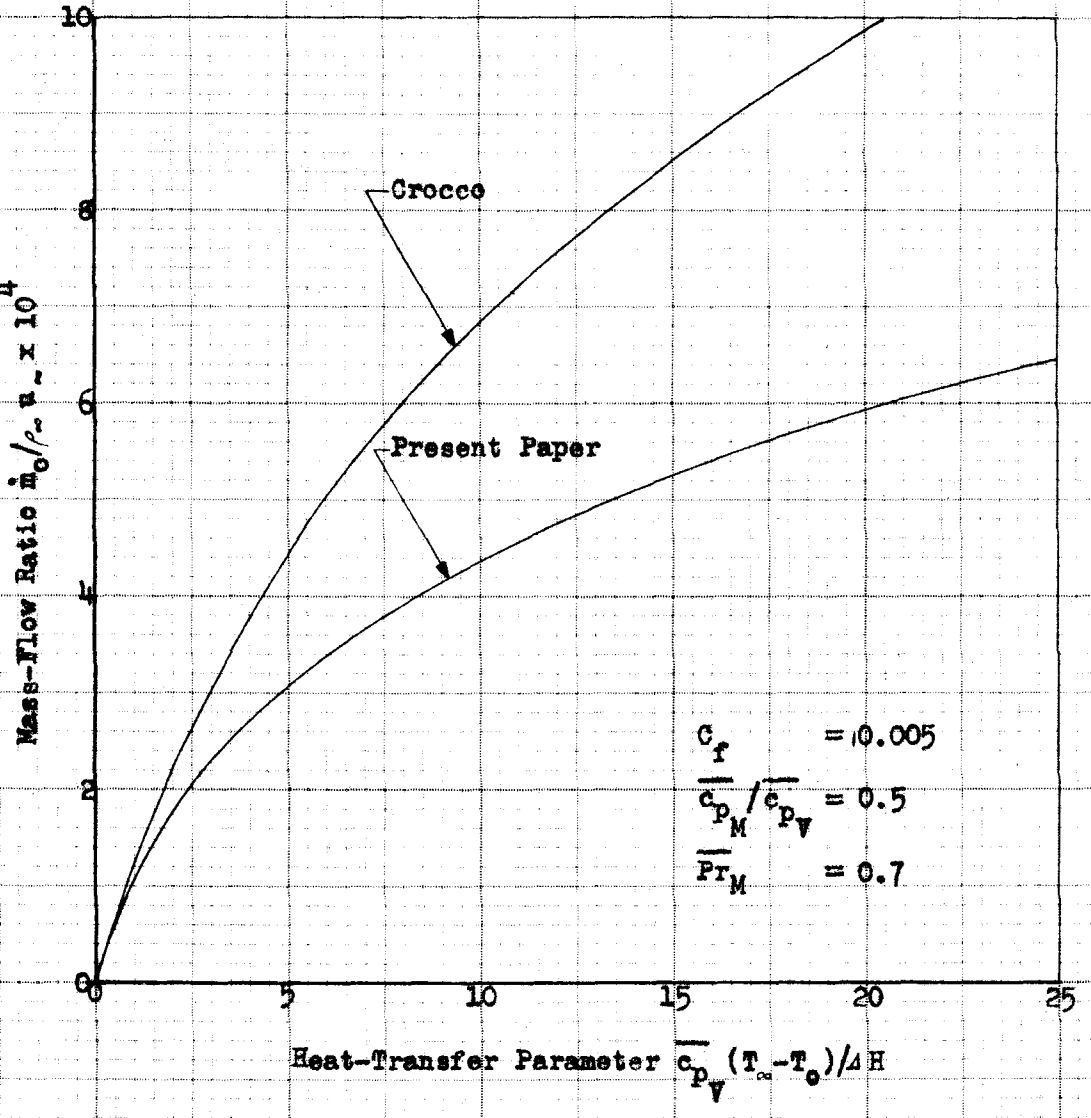

Figure 17. Mass-Flow Ratio vs Heat-Transfer Parameter as Predicted by Crocco and Present Paper

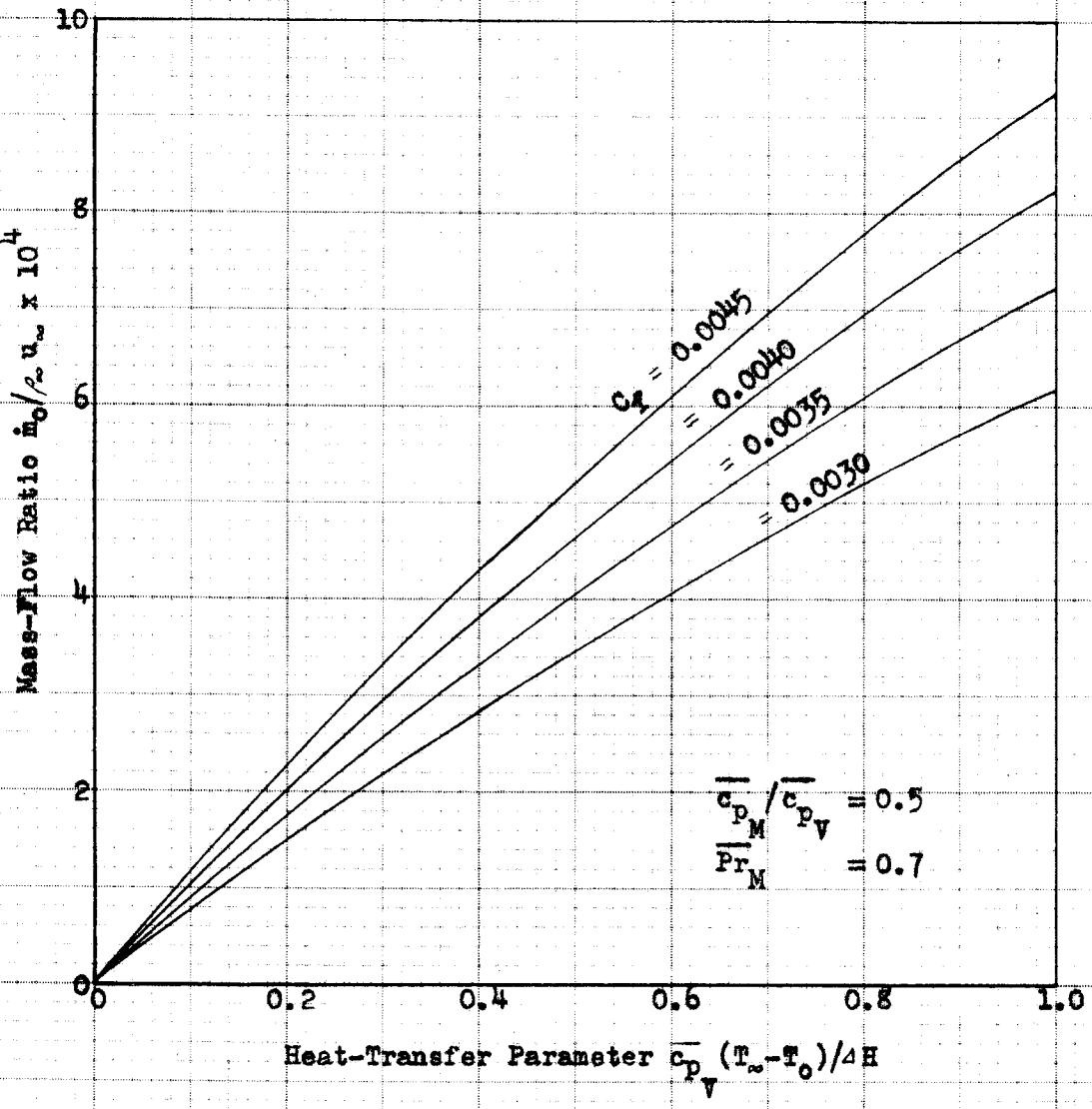

Figure 18. Mass-Flow Ratio vs Heat-Transfer Parameter for Water Evaporating into Air Stream

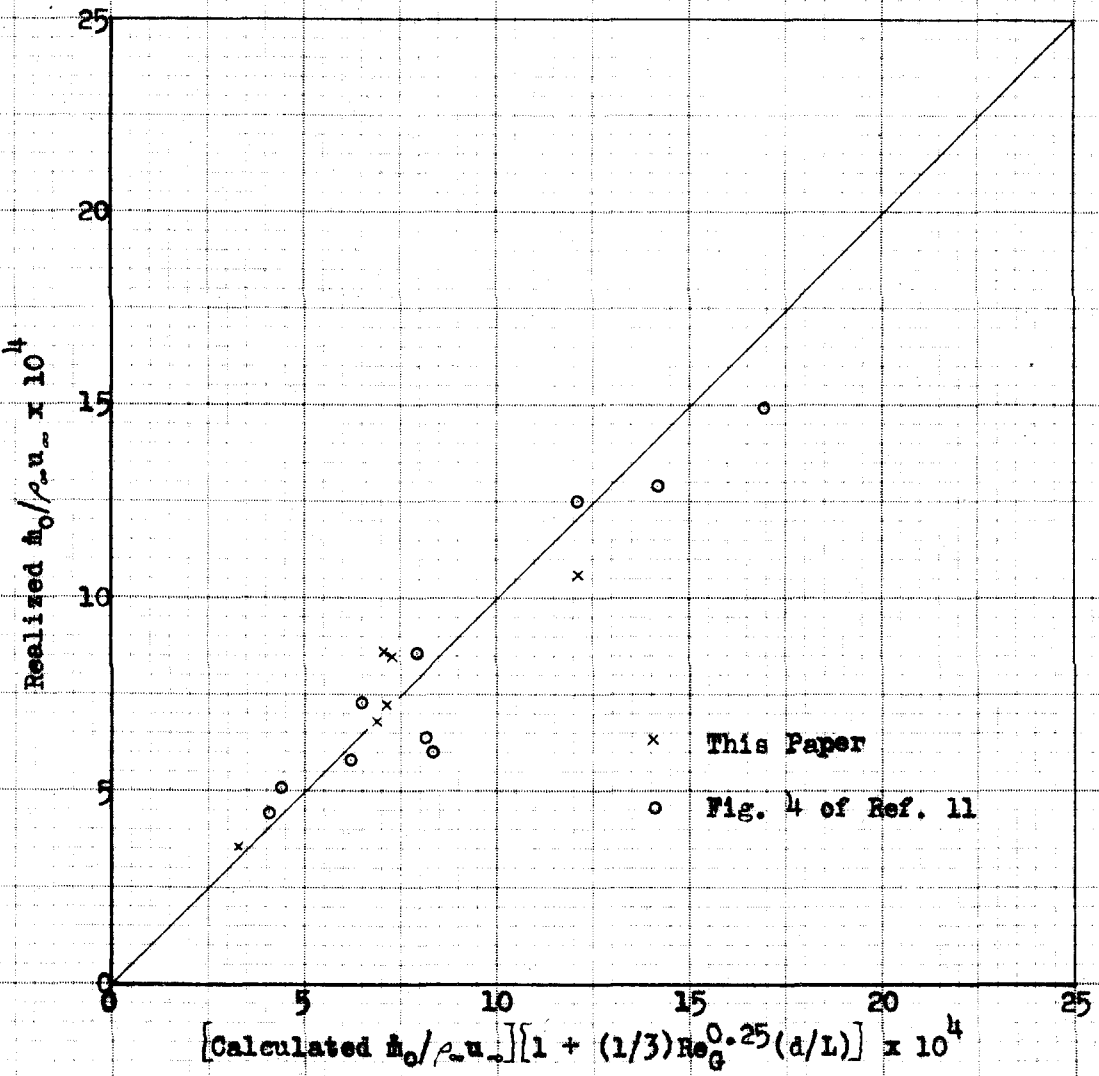

Figure 19. Comparison of Realized Mass-Flow Ratio with Calculated Mass-Flow Ratio